NASA TECHNICAL MEMORANDUM 107637
AVSCOM TECHNICAL REPORT 92-B-009

SCALE EFFECTS ON THE TRANSVERSE TENSILE STRENGTH OF GRAPHITE EPOXY COMPOSITES

T. K. O'Brien and S. A. Salpekar

Presented at the 11th ASTM Symposium on Composite Materials: Testing and Design; Pittsburgh, PA; May 4-5, 1992

June 1992

National Aeronautics and Space Administration

Langley Research Center
Hampton, Virginia 23665-5225

US ARMY AVIATION SYSTEMS COMMAND
AVIATION R&T ACTIVITY

SUMMARY

The influence of material volume on the transverse tensile strength of AS4/3501-6 graphite epoxy composites was investigated. Tensile tests of 90 degree laminates with 3 different widths and 5 different thicknesses were conducted. A finite element analysis was performed to determine the influence of the grip on the stress distribution in the coupons and explain the tendency for the distribution of failure locations to be skewed toward the grip. Specimens were instrumented with strain gages and extensometers to insure good alignment and to measure failure strains. Data indicated that matrix dominated strength properties varied with the volume of material that was stressed, with the strength decreasing as volume increased. Transverse strength data were used in a volumetric scaling law based on Weibull statistics to predict the strength of 90 degree laminates loaded in three point bending. Comparisons were also made between transverse strength measurements and out-of-plane interlaminar tensile strength measurements from curved beam bending tests. The significance of observed scale effects on the use of tests for material screening, quality assurance, and design allowables is discussed.

KEYWORDS: Composite Material, Graphite Epoxy, Transverse Tensile Strength, Delamination, Matrix Crack, Scale laws, Weibull statistics.

INTRODUCTION

Transverse tensile strength tests are commonly conducted on unidirectional laminates oriented at 90 degrees to the load axis. These data are routinely generated for material screening and quality assurance. However, these data have also been used as in-plane transverse strength properties in phenomenological strength criteria and to identify "first ply failure" in progressive damage models [1,2]. Furthermore, these data are often used to estimate the out-of-plane strength of the composite in delamination failure criteria [3,4]. However, the volume of material used in the test specimen may influence the transverse tensile strength of the composite, and hence, may influence the accuracy of the predictions generated.

The purpose of this study was to determine if a volume sensitive scale effect was present in transverse tensile strength data generated using 90 degree tensile coupons. Tensile tests of AS4/3501-6 graphite epoxy were conducted using the procedure described in ASTM standard D3039-76 where applicable. This standard recommends a specimen width of 1.0 inch and a specimen thickness between 0.02 to 0.10 inches for 90 degree tensile tests, which for a typical 5 mil graphite epoxy prepreg, corresponds to a 4-ply to 20-ply laminate. In this study, configurations were tested that had volumes both less than, and greater than, the recommended configurations. The 90 degree laminates tested had 3 different widths and 5 different thicknesses. Specimens were instrumented with strain gages to insure good alignment and to measure failure strains. A finite element analysis was conducted to determine the influence of the grip on the stress distribution in the coupons and the tendency for the distribution of failure locations to be skewed toward the grip.

MATERIALS AND SPECIMEN PREPARATION

Twelve-inch-square panels of unidirectional AS4/3501-6 graphite epoxy were layed up from 5 mil prepreg and cured in an autoclave according to the manufacturer's recommended curing cycle. Four panels were manufactured, each having a different thickness corresponding to the number of plies (4,8,16,32) used

during the lay up. In addition, three 64-ply panels were manufactured.

After manufacture, each panel was C-scanned to assess the panel quality. The C-scans for the 4,8,16 and 32-ply panels all indicated good quality panels. Hence, these panels were each cut into 9 specimens, 3 each of 3 different widths (0.5, 1.0, & 2.0 inches) according to the schematic shown in fig.1. Ultrasonic C-scans for the first 64-ply panel indicated extensive voids in the center of the panel. Two additional 64-ply panels had similar C-scans. Hence, a limited number of specimens with 0.5, 1.0, and 2.0 inch widths were cut from the regions of these three panels, away from the center, where the C-scan indicated the panels were free of voids.

All test specimens were 11.5 inches long. The specimens were cut from each panel using a diamond wheel saw blade to minimize the potential for machining flaws. The specimen widths were measured with flat nose calipers in three locations along the specimen length and averaged to obtain the average specimen width. The specimen thicknesses were measured with ball point calipers in the middle of the specimen width, and near the specimen edges, at three locations along the specimen length and averaged to obtain an average specimen thickness. The average laminate thickness for all specimens tested was divided by the number of plies to obtain an average ply thickness. The average ply thicknesses are shown in table 1. The product of the average ply thickness and the manufacturer's supplied fiber density (1.8 g/cm^3) was divided into the fiber aerial weight (149 g/m^2) for AS4/3501-6 to estimate fiber volume fractions (table 1).

Because ASTM standard 3039-76 does not specify the size of the strain measuring device, three different strain measuring instruments were utilized to measure transverse failure strain. These instruments had different gage sizes to assess the influence of gage size on measured failure strains. One inch gage length extensometers and two different size strain gages, with 0.062 and 0.125 inch gage lengths, were mounted on the test coupons. The number and location of strain gages and extensometers varied depending on the specimen width and thickness. Each size specimen (i.e., each unique combination of width and thickness), had one specimen instrumented in a bending check configuration to assess the accuracy of the specimen alignment in the grips and two specimens instrumented in a gage size effect configuration to assess the influence of the gage length on measured failure strains. For example, figure 2 shows the two configurations used for the 4,8,16, and 32-ply specimens for both narrow (0.5 in.) and wide (1.0,

2.0 in.) laminates. The 64-ply laminates were instrumented with back-to-back 0.125 inch gage length strain gages only.

EXPERIMENTAL PROCEDURE

All specimens were tested in servo-hydraulic load frames by the same operator. The 4,8,16, and 32-ply coupons were mounted in machines with bolted, symmetric flange grips resembling a tuning fork when viewed from the edge as shown in figure 3. The gage length shown in figure 3 is significantly shorter than the gage length used for testing. Shims were placed symmetrically on either side of the specimen to reduce the flexure in each flange needed to grip the specimen as the bolts were tightened. Instead of bonding tabs onto the specimens as recommended in ASTM D3039-76, cellulose acetate sheets were placed next to the untabbed specimen surfaces. These thin sheets helped to reduce the probability of surface scratches from the serrated grip faces causing premature failure and to soften the transition from a constrained biaxial stress state at the grip line to a uniaxial stress state in the test section. The bolt torque was kept low (between 90 and 300 in-lbs) to just prevent slippage. For the thinnest and narrowest specimens with anticipated low failure loads, a 500 pound load cell was placed in series with the 5000 lb load cell to monitor the failure load more accurately. The 64 ply coupons were mounted in hydraulic grips. The hydraulic grip pressure was kept low (1000 psi) to minimize the possibility of inducing any local damage to the specimen surfaces.

All specimens were loaded in the grips such that the distance between the ends of the top and bottom grips was 7.0 inches. ASTM standard D3039-76 recommends a strain rate between 0.01 to 0.02 in./in/min in the gage section. For the specimens tested in this study, this corresponds to a minimum load rate of 125 pounds/min for the thinnest, narrowest and most compliant specimens and a maximum load rate of 16,000 pounds/min for the thickest, widest and stiffest specimens tested in this study. Specimens were tested in load control at a loading rate of either 100 or 500 pounds per minute, depending on their width and thickness, until the specimen failed. The thinner and narrower specimens were loaded at the lower rate. The load and strains were recorded in real time on X-Y-Y' recorders during the test. The bending test configuration specimen was run first for each unique specimen width and thickness combination. After the specimen failed, but before the specimen was removed from the grips, the break length from the top of each grip to

the failure location was measured, as well as the specimen width and thickness in the local vicinity of the failure.

EXPERIMENTAL RESULTS

Transverse Tensile Strength Measurements

The failure loads for all the specimens tested are shown in table 2. Several specimens failed at the nip point at the end of the grip (hereafter referred to as the grip line) or within the grip itself. These failures were indicated as grip failures in table 2. The data from these grip failures were not considered to be representative of the transverse tensile strength of the material, and hence, were not included in the determination of mean strengths.

For each specimen, the failure load was divided by the average specimen width and thickness to obtain a nominal transverse tensile strength. Nominal transverse tensile strengths are tabulated in table 3. Failure loads were also divided by the local width and thickness measured in the vicinity of the failure location to obtain a local transverse tensile strength. Local transverse tensile strengths are tabulated in table 4. Local strengths were not tabulated for specimens that failed in more than one location simultaneously. The local strength measurements averaged between 5 and 6% higher than the nominal strength measurements.

Transverse Failure Strain

Transverse tensile failure strains are tabulated in tables 5-7. Some variation in measured failure strain was noted for the different size strain gages and the extensometers. The average variation in failure strain measurements made using the small and large strain gages located at two different locations within the central test section on the same side of the specimen was 9.9%. In one case the variation in failure strains measured using the small and large gage were as high as 25%. The variation in failure strain measurements made using 0.125 in. gage length strain gages and 1.0 in. gage length extensometers located at two different locations within the central test section on the same side of the specimen was 6.9%. In one case the variation in failure strains measured using the extensometer and the strain gage was as high as 9.4%.

Although large variations in measured failure strains with gage size were noted on individual specimens, there was no direct correlation between the gage size and the measured failure strain.

For example, the smaller gages did not always yield the higher strain measurement on each specimen, or vice versa. Furthermore, there was very little variation between mean values of failure strains measured using different size gages as noted in table 8.

Failure Location Influence on Strength

In addition to the grip failures, a large percentage of the specimens failed outside of the grip region but within the local vicinity of the grip. ASTM standard D3039-76 states that a significant fraction of failures within one specimen width of the grip shall be cause to examine the gripping method. Figure 4 shows the nominal transverse tensile strength plotted against the break length normalized by the specimen width. The distribution of break lengths was skewed toward the grip, with nearly half of all the specimens tested failing within one specimen's width distance from the grip line (Break length/width<1). However, these data have roughly the same magnitude and range as the data for the remaining specimens where failure occurred in the central region of the test section. Hence, it was assumed that the data from all the tests where failure was not at the grip line, or within the grips, were valid strength measurements. The validity of this assumption will be discussed later after examining the results of the finite element analysis of specimens including the local region near the grips.

Bending Influence on Strength

Figure 5 shows the nominal transverse tensile strength for each thickness tested plotted versus percentage variation in identical size back-to-back strain gage readings for the bending test configuration specimens. Only one half of the specimens had variations less than 5% as mandated by ASTM standard D3039-76. However, the magnitude and range of the measured strengths from specimens with back-to-back failure strain variations greater than 5% was similar to the magnitude and range of measured strengths where the variation was less than 5%. Furthermore, the average variation in failure strain measurements made using identical size gages located at two different locations within the central test section on the same side of the specimen was 2%. In one case the variation in failure strain between two identical gages was as high as 4.5%. Hence, the lack of repeatability in the failure strain measurements for any unique size gage may also contribute to the apparent variations in back-to-back strain measurements shown in

figure 5. Therefore, it was assumed that the data from all the tests were valid measurements of the transverse tensile strength.

The strain gages used in the bending configuration were mounted near the mid-plane of the test section. However, as noted in ASTM standard D3039-76, the maximum bending moment will occur near the grip. In the absence of back-to-back strain data in this region, the significance of an out-of-plane misalignment, d, on the surface ply tension stress due to combined extension and bending may be estimated as

$$\sigma = P\left(\frac{1}{bt} + \frac{6d}{bt^2}\right) \tag{1}$$

where b is the specimen width and t is the specimen thickness. This equation indicates that for a given misalignment, d, the surface ply tension stress increases linearly with decreasing specimen width and increases quadratically with decreasing specimen thickness. Hence, if misalignment is significantly influencing the test results, a trend of increasing strength with increasing thickness and width should be evident. This trend is just the opposite of the trend of decreasing strength with increasing thickness or width that would be evident if a flaw sensitive volume effect is influencing failure.

ANALYSIS

A two dimensional plane stress finite element analysis was conducted to assess the severity of the transition from a constrained biaxial stress state at the grip line to a uniaxial stress state in the test section for several composite layups. One purpose for conducting this analysis was to determine if the St. Venant's theory rule-of-thumb from classical isotropic elasticity theory, i.e. that a uniaxial stress state exists at a distance of one specimen width from the grip line, was valid for orthotropic laminates. Another purpose for conducting this analysis was to determine if the influence of the grip region on the stress state in tensile specimens could explain the observed tendency for the distribution of failures to be skewed toward the grip line in the 90 degree tensile tests.

Figure 6 shows the typical dimensions of the specimen that was modeled. The axial and transverse (u and v) displacements were constrained at one end to simulate the grip and a uniform stress, σ_0, was applied on the opposite end to simulate the central region of the test section away from the grip. The model included 2400 eight noded isoparametric parabolic elements with 7481 nodes. All

elements were uniform in size (0.025 in by 0.025 in.). Two degrees of freedom (u and v) were assumed at each node.

The distribution of the normalized stress transverse to the load direction, σ_y/σ_0, in the vicinity of the grip (x/w=0) is shown in figure 7. The transverse stress, σ_y, is highest in the center of the specimen width at the grip line, where it reaches 30 percent of the remote axial stress, σ_0. However, as shown in figures 7 and 8, this transverse stress vanishes at a distance of 1/4 of the specimen width from the grip line (x/w=0.25). The decay length for normalized σ_y in the center of the laminate width is similar to that observed for zero degree and cross-ply orthotropic laminates, but is only half as long as the decay length obtained for a quasi-isotropic laminate (fig.8). Both these decay lengths are less than the one specimen width (x/w=1.0) rule of thumb typically assumed to be necessary to achieve a uniaxial stress state.

The distribution of the normalized axial stress, σ_x/σ_0, in the vicinity of the grip is shown in figure 9. The axial stress, σ_x, is highest at the edge of the specimen width at the grip line, where its magnitude exceeds the remote axial stress, σ_0. Therefore, if the 90 degree specimens were perfectly homogeneous and free of flaws all failures should occur at the grip line. The fact that only a few specimens failed in the grips, and the majority of the tests failed within the test section, is evidence that inherent flaws were present in the microstructure.

The distribution of the normalized shear stress, τ_{xy}/σ_0, in the vicinity of the grip is shown in figure 10. The shear stress, τ_{xy}, distribution is asymmetric across the specimen width, with the highest magnitudes occuring along the grip line at the specimen edges. These stresses may also contribute to grip failures along the grip line.

Although the axial and shear stresses predicted from the analysis are greatest along the grip line at the specimen edges, both the axial and shear stresses decreased rapidly with distance from the grip line as shown in figures 11 and 12. The axial stress, σ_x, at the specimen edge decreases to the remote axial stress level at a distance of less then one tenth the specimen width (x/w = 0.1), where it decreases before eventually increasing to the remote stress level at approximately 1/4 of the specimen width from the grip line (fig.11). A similar trend in normalized axial stress versus distance from the grip is observed for a zero degree orthotropic laminate (fig.11). In contrast, a quasi-isotropic laminate does not

recover the remote axial stress until one full specimen width from the grip line (fig.12), which is consistent with the St. Venant's rule of thumb based on isotropic elasticity. The shear stress, τ_{xy}, at the specimen edge decreases to zero at a distance of less then one tenth the specimen width (x/w = 0.1), where it oscillates with very small magnitudes until becoming identically zero at approximately 1/4 of the specimen width from the grip line (fig.13).

RESULTS AND DISCUSSION

Figures 14 and 15 show the nominal transverse tensile strength data from table 3 plotted as a function of the specimen thickness and width, respectively. As shown in fig.14, the 8-ply laminates appear to be the strongest, followed by the 4 and 16-ply laminates, with the 32-ply and 64-ply laminates yielding similar, but on average, slightly lower strengths. All five specimen thicknesses had similar average ply thicknesses and fiber volume fractions (table 1). As shown in fig.15, there was no apparent variation in strengths between the 0.5 inch, 1.0 inch, and 2.0 inch wide specimens.

Figure 16 shows the nominal transverse tensile strength data plotted as a function of the net cross sectional area of the specimen. All these data represent strength measurements on specimens with 7.0 inch test section lengths. Thus, a constant cross sectional area also corresponds to a constant volume of material stressed. As noted earlier, there was a lot of scatter in these data. However, a trend of decreasing strength with increasing cross sectional area, and hence increasing volume, is evident.

The trend of decreasing strength with increasing material volume observed in fig.16 may be interpreted as a volumetric dependence on strength due to the presence of imperfections, flaws, inhomogeneities, or local discontinuities in the microstructure of the material. Local microcracks in the matrix, and/or local fiber-matrix disbonds, are the most likely inherent flaws. If no flaws are present, the stress analysis would indicate that all failures should occur at the grip line, assuming a rigid clamped boundary actually exists at the grip. However, the specimen may not be rigidly clamped at the intersection of the specimen edge and grip line as assumed in the analysis, but may achieve a zero transverse displacement more gradually due to the acetate film insert. However, because of the tendency for the axial stress to be highest near the free edges in the vicinity of the grip line, any flaws in this region may be more critical than in the remainder of the laminate. This may explain why

nearly half of all specimens tested failed within one specimen's width distance from the grip line (fig. 4). Furthermore, if flaws associated with the edge were most critical, there should be little difference in the strength of specimens with identical thickness but with different widths. This appeared to be the case as shown in figure 15.

The presence of a volumetric dependence on the transverse tensile strength measured using 90 degree tensile coupons indicates that this test does not measure a generic property of a graphite epoxy material, but rather, characterizes a flaw sensitive response of an inhomogeneous composite lamina. Therefore, 90 degree tensile tests used for material screening or quality assurance purposes should always be conducted on the same size specimen to obtain valid comparisons. Furthermore, any application of these measurements to predict transverse failure in 90 degree plies of laminates, or to predict interlaminar failure, should incorporate this flaw size sensitivity by scaling these measurements based on the local volume that is stressed. One method of doing this is to use a volumetric strength model based on Weibull statistics.

Transverse Strength Scaling

Weibull assumed an extreme value, or "weakest link", distribution for material strength by developing a two parameter function for the probability of failure at a given stress level, $P(\sigma)$, of the form

$$P(\sigma) = 1 - \exp^{-\left(\frac{\sigma}{\sigma_c}\right)^m} \qquad (2)$$

where σ_c is the location parameter known as the characteristic strength, and m is the shape parameter known as the Weibull slope [5]. The location parameter, σ_c, provides a measure of the central tendency of the distribution, similar to the mean for a normal distribution. The shape parameter, m, provides a measure of the scatter in the distribution, with a small value of m corresponding to a large amount of scatter in the data. Equation (2) may also be recast into an equation of the form

$$y = m \ln\sigma + b \qquad (3)$$

where

$$y = \ln\left[\ln\left(\frac{1}{1- P(\sigma)}\right)\right] \quad (4)$$

and

$$b = - m \ln\sigma_c \quad (5)$$

Then, by assuming a probability of failure corresponding to a median ranking of the data

$$P(\sigma) = \frac{(i-1) + 0.7}{n + 0.4} \quad (6)$$

where n is the total number of data points in the sample and i is the number of the data point in ascending order from 1 to n, a least squares regression fit of the logarithmic eq (3) may be performed to determine m and σ_c.

Because m characterizes the extent of scatter inherent in the ultimate strength measurement, a large number of tests are required to determine m for a given material system (see appendix). Ideally, these tests should be conducted on a single configuration. Since a maximum of 4 replicates were obtained for any single configuration tested in this study, it was not possible to determine a unique value of m from any unique configuration tested. However, because the strength distributions for different volumes overlapped significantly (fig.16), and because the mean strengths decreased gradually with volume compared to the scatter in the data (fig.16), all the 90 degree test results were combined into one data set to estimate m.

Table 9 lists strength data for the 4,8,16,32 and 64-ply laminates in ascending order with their associated probability of failure. The transverse tensile strength distribution of these data is plotted in fig. 17. This set of 33 data points yields a characteristic strength of 8.87 ksi and a shape parameter, m, of 7.63. In reference 6, a value for m of 7.68 was determined from a set of 114 ninety degree tension tests for T300/5208, a graphite epoxy material system similar to the AS4/3501-6 material tested in this study. An identical m value was also obtained in ref.6 for T300/5208 from 135 flexure strength tests. The results from ref.6 suggest that the Weibull shape parameter is a material constant, independent of test configuration and the volume of material.

Several other estimations for the shape parameter, m, were performed by omitting selected data points that were of questionable validity. First, three data points corresponding to specimens that failed within one tenth of the specimen width from

the grip line (table 9) were omitted because the shear stresses near the grip may have influenced these failures (fig.13). The remaining 30 data points left after omitting these near-grip failures were assigned a new median rank using eq(6) and were fit to eq(3) yielding a shape parameter, m, of 7.67. Hence, omission of these near-grip failures had no significant influence on m. Second, all five data points from the 4-ply specimens were omitted (table 9) because there was some potential influence of misalignment as evidenced by lower strengths for the 4-ply compared to the 8-ply laminates (fig.14). The remaining 28 data points left after omitting the 4-ply laminates from the original data set were assigned a new median rank using eq(6) and were fit to eq(3) yielding a shape parameter, m, of 7.04. Finally, strength data from both the near grip failures and the 4-ply laminates were omitted from the original data set. The remaining 25 data points were assigned a new median rank using eq(6) and were fit to eq(3) yielding a shape parameter, m, of 7.02. Again, omission of the near-grip failures had no significant influence on m. The transverse tensile strength distribution of these data is plotted in fig.18.

Other researchers have recommended flexure tests as an alternative to 90 degree tensile tests for determination of transverse tensile strength. For example, a three point bend flexure test on a 90 degree specimen has been proposed [7] in which only a small volume of material near the mid-span on the tension side of the beam is subjected to a high stress resulting in a more local failure. In ref.[8], 90 degree and off-axis flexure tests were performed on AS4/3501-6 laminates. Figure 19 shows the nominal transverse tensile strength data from 90 degree tensile tests plotted as a function of the net volume, corresponding to the cross sectional area of the specimen multiplied times the 7.0 inch test section length. Also shown in fig.19 is the apparent transverse tensile strength measured from 90 degree specimens subjected to three point bending [8]. The flexure strength data were plotted versus an assumed small local volume, shown in figure 20. This arbitrarily chosen small (7.02×10^{-6} $in.^3$) local volume corresponds to a local highly stressed area on the tension side of the beam, below the central load nose, consisting of one square ply thickness, h^2, (where h=0.0053 in.) multiplied times the 0.25 inch beam width [8]. As shown in fig.19, the apparent transverse strength measured from the flexure test is higher than the data from the smallest 90 degree tension specimens tested.

Weibull postulated that the values of the mean ultimate strengths for two different volumes, V_1 and V_2, of the same material, will obey the following scale law [5]

$$\frac{(\sigma_{ult})_1}{(\sigma_{ult})_2} = \left(\frac{V_2}{V_1}\right)^{1/m} \qquad (7)$$

This equation was used to estimate the strength for the three point bend flexure specimen using the transverse tensile strength data and the Weibull shape parameter, m.

First, the transverse tensile data were grouped according to volume. Table 10 shows different combinations of specimen width and thickness corresponding to similar cross sectional areas, and hence, similar volumes. For example, the 2.0 inch wide 4-ply laminate, the 1.0 inch wide 8-ply laminate, and the 0.5 inch wide 16-ply laminate all have similar volumes and are identified as case D. An average volume for similar cases B-H is tabulated in table 11. Case A in table 11 lists transverse tensile strengths obtained from the three point bend flexure tests conducted on 90 degree specimens in ref. 8.

Then, the minimum, maximum, and average strength, $(\sigma_{ult})_2$, tabulated in table 11 for each case, was substituted in eq(7) to predict the minimum, maximum, and average strength for the flexure specimens, $(\sigma_{ult})_1$. In eq(7), the volume, V_2, corresponds to each 90 degree tension case in table 11 and V_1 corresponds to the small local volume, 7.02×10^{-6} in.^{3}, for the three point bend specimen. Initially, the shape parameter, m=7.63, obtained from the logarithmic curve fit of the all transverse tensile test data was used in eq(7). As shown in fig.21, the predicted strengths from each 90 degree test volume type were similar, indicating that the scaling law may be used to correlate transverse tensile strengths from one configuration to another. However, each of the predicted strengths was nearly three times as high as the measured flex strengths from the three point bend tests. One reason for this discrepancy may be that the highly stressed volume assumed for the beam was unrealistically small.

Next, it was assumed that any portion of the beam that sees a tensile stress would have some finite probability of failure if the beam has inherent microstructural flaws similar to the tensile specimens. Therefore, a larger volume was assumed for the local volume, V_1, corresponding to the product of one half of the measured 24-ply beam depth, the beam span, 2L, of 2.1 inches, and the beam

width, w, of 0.25 inches (fig.20). This large local volume also represents an upper bound of possible choices for tensile failure. As shown in fig.22, the predicted strengths assuming this larger local volume for the beam agree well with the measured flex strengths from the three point bend tests.

Finally, the three point bend test strength was predicted using the large local volume and the shape parameter, m=7.02, determined from the original data set minus the near-grip and 4-ply laminate strength data. As shown in fig.23, the predicted strengths assuming this larger local volume for the beam and the lower value of m agree well with the measured strengths. Hence, the Weibull scaling law of eq(7) is more sensitive to the local volume chosen than to small variations in the Weibull shape parameter.

Fig. 24 shows the nominal transverse tensile strength data for the 90 degree tensile tests, and the three point bend specimen assuming the larger local volume, plotted as a log function of the volume of material stressed. As noted earlier, there was a lot of scatter in these data. However, a trend of decreasing strength with increasing cross sectional area, and hence increasing volume, is evident.

Comparison of in-plane and out-of-plane strength

Transverse tensile strength measurements are commonly used to estimate the out-of-plane interlaminar tensile strength, $(\sigma_z)_{ult}$ [4]. Recently, however, other test methods have been proposed to measure the out-of-plane tensile strength directly. Perhaps the most promising methods involve testing curved beams under bending [9-11]. These curved beam tests appear to be especially sensitive to the presence of voids, resin pockets, and resin rich interlayers. These macroscopic inhomogeneities typically occur as a result of the difficulty achieving a uniform pressure in the curved region of the beam during manufacture [8,9]. Macroscopic inhomogeneities (such as voids, etc.) are easily detected in flat panels using ultrasonic C-scans, but are not easily detected using the same techniques in laminates with curved regions. Researchers have reported two distinct sets of data from curved beam tests: (1) a set with higher strengths where the inherent flaws are in the microstructure only, as assumed for tension and three-point bend specimens cut from good quality panels screened using ultrasonics, and (2) a set with lower strengths where voids and other inhomogeneities are evident in the macrostructure as observed by post mortem inspection of polished sections [11].

In reference 11, out-of-plane strength was measured using unidirectional curved beams of AS4-3501-6 graphite epoxy. The data from these tests corresponding to microstructural flaws only may be reasonably compared to the transverse strength data from tensile tests and three point bend tests. For curved beams subjected to bending loads, the radial stress in the curved portion of the beam, predicted from finite element and elasticity analyses [11], is tensile throughout the beam thickness, reaching a maximum at a location slightly off the centerline towards the inner radius as shown in the lower left sketch in figure 25. Furthermore, as shown in the lower right sketch in figure 25, for any given location through the thickness (r = constant) the radial stress is tensile and relatively constant in the curved portion of the beam. Therefore, it was assumed in this study that the large local volume, where a flaw induced failure had a finite probability of occuring, consisted of the entire cross section of the curved portion of the beam times the beam width. The length of the small portion of the straight arms that had tensile stresses was unknown, and hence, was neglected. For the 0 degree curved beam configuration used in ref [11] the large local volume is given by

$$V = \frac{\pi w t}{4}(t + 2r_i) \tag{8}$$

where w, t, and r_i are the width, thickness, and inner radius of the curved region respectively.

Figure 26 compares strength data generated from three curved beam configurations (corresponding to three unique combinations of width, thickness, and inner radius in 16 and 24-ply unidirectional curved beams) to three point bend test data as a function of the material volume that is stressed. All these data consist of similar local volumes and strengths. The local volumes would agree even closer if the small tensile stressed region in the straight arms of the curved beams had been included. This comparison suggests that the transverse tensile strength measured from the small three point bend specimens may be used to estimate the out-of-plane interlaminar tensile strength in good quality curved beam sections that do not contain macroscopic inhomogeneities. A more general approach for scaling these strengths measurements, however, would be to apply a scaling law based on Weibull statistics.

In ref.11, the 17 out-of-plane strength measurements generated from the 3 curved beam bending configurations that yielded good quality parts were combined and assigned a median rank

using eq(6) and were fit to eq(3) to estimate the Weibull parameters for out-of-plane strength. A shape parameter, m, of 7.75 was obtained, which is similar to the 7.63 value obtained from combining the 90 degree tension test results in this study and the 7.68 value obtained in ref.6 from both tension and flex tests on T300/5208 graphite epoxy.

Fig. 27 compares strength data generated from the three good quality curved beam configurations from ref[11] to the transverse strength data generated from tensile tests in this study as a log function of the material volume that was stressed. As noted earlier, there was a lot of scatter in these data. However, a trend of decreasing strength with increasing volume, is evident.

The Weibull scaling law (eq.7) was used to determine if the transverse tensile strength data could be used to predict the out-of-plane strength measured by the curved beam bending tests. The minimum, maximum, and average strength, $(\sigma_{ult})_2$, values tabulated in table 11 for each case were substituted in eq(7) to predict the minimum, maximum, and average strength for the 16 ply curved beam with a 0.2" inner radius, $(\sigma_{ult})_1$. In eq(7), the volume, V_2, corresponds to each 90 degree tension case in table 11 and V_1 corresponds to the volume of the curved section of the beam, 0.0293 $in.^3$. The shape parameter, m=7.63, obtained from the logarithmic curve fit of the all transverse tensile test data was used in eq(7). As shown in fig.28, the predicted strengths agreed well with the measured out-of-plane interlaminar tensile strengths shown as case A. Predictions for the other 16 and 24-ply curved beams also showed good agreement with the measured strengths.

Any one of the three tests examined in this study (90 degree tension, three point bend, and curved laminate) may be used to characterize the microstructural flaw sensitivity inherent in matrix dominated strength properties. Strengths measured from any one of these tests could be used in a Weibull based scale law to predict matrix dominated failures in laminates with non-uniform stress fields. However, a large number of tests is required to accurately determine the Weibull shape parameter no matter which test is used (see appendix). Therefore, a three point bend test may be the most desirable for this purpose because it requires a small amount of material and is easier to test than the transverse tension and curved beam bending tests. However, as noted in ref.11, the curved beam bending test may also be needed to ascertain the quality of curved structural members that may have macroscopic voids and

inhomogeneities that cannot be easily detected using classical ultrasonic NDE methods.

In Situ Strength of Laminate Plies

Previously, researchers have noted that the in situ strength of 90 degree and off-axis plies in composite laminates depends on the laminate layup, stacking sequence, and ply thickness [12]. The observed ply thickness dependence may simply reflect the dependence of transverse strength on material volume noted in this study. Therefore, if a strength criterion is used to determine in situ ply strength, an appropriate local volume in eq(7) must be identified to apply the Weibull scaling law.

In composite laminates with arbitrary layups and stacking sequences, the in-plane stresses that cause matrix cracking will deviate from the laminate theory prediction near the straight edge. For example, figure 29 shows the distribution across the laminate width of the in-plane normal stress transverse to the fiber direction, σ_{22}, for $(0/\theta/-\theta)_S$ graphite laminates subjected to a total (mechanical + thermal) axial strain of 0.01, assuming a ΔT of -156°C (-280°F), where θ = 15, 30, and 45 degrees [13]. The values in the interior, corresponding to (b-y)/h = 5, agree with the values calculated from laminated plate theory, where the normal stresses in the 45 degree case are tensile and the normal stresses in the 15 and 30 degree cases are compressive. However, near the free edge, (b-y)/h = 0, the magnitude of the tensile stresses increases for the 45 degree case and the sign of the normal stresses change from compression to tension for the 15 and 30 degree cases. Hence, the volume of material that is highly stressed corresponds to a small volume represented by the ply thickness times an appropriate boundary region. Transverse strength data measured on larger volume specimens intended for use in a failure criteria should be scaled using eq(6) to accurately predict matrix cracking.

Following the three point bending and curved beam examples cited earlier, the appropriate volume for the cases shown in fig.29 would correspond to the total volume of material that is stressed in tension. For the 45 degree case, this volume would correspond to the entire laminate width times the ply thickness and gage length. However, for the 15 and 30 degree cases this volume would correspond to only a small portion of the laminate width near the edge, on the order of one ply thickness or less, times the ply thickness and gage length. Similar volume scaling of shear strengths

may also be needed if a combined stress failure criteria is required to predict matrix cracking. Furthermore, if the non-uniform stress field includes a stress singularity, as opposed to a finite stress concentration implied by the example in fig. 29, a fracture mechanics characterization of matrix failure may be more useful. The volume dependence could be characterized through a parameter such as the strain energy release rate, which depends on the ply thickness, and hence, directly incorporates the volumetric sensitivity in the measured fracture toughness. In these cases, a fracture mechanics based prediction of matrix dominated failures may be more appropriate.

CONCLUSIONS

Based on the testing and analysis that was conducted in this study, the following conclusions were reached:

1. The classical rule of thumb assuming that a distance of one specimen width from the grip line is required to achieve a uniaxial stress state in a tension test is conservative for 0 degree, 90 degree, and 0/90 composite laminates.

2. The transverse tensile strength of a composite laminate depends on the volume of material that is stressed in the test used to measure this property. This volume dependence reflects the presence of inherent flaws in the microstructure of the lamina.

3. Ninety degree tensile tests used for material screening or quality assurance purposes should always be conducted on the same size specimen to obtain valid comparisons.

4. Strengths measured from 90 degree tensile tests, 90 degree three-point bend tests, and 0 degree curved beam bending tests all characterize the matrix dominated strength of the composite and differ in magnitude only because of their difference in volumes. Any one of these tests could be used in a scale law based on Weibull statistics to predict matrix dominated failures in laminates with non-uniform tensile stress distributions.

5. If ninety degree tensile tests are used to generate transverse tension strength allowables for strength-based failure criteria, or for use in progressive failure criteria, the transverse tensile strength should be characterized using Weibull statistics,

and the ultimate strengths should be scaled to the appropriate volume of interest. Preliminary analysis indicates that for non-uniform stress field with finite stress concentrations, the maximum tensile stress and the total volume of material stressed in tension should be used in a scale law for transverse tensile strength to predict matrix cracking or delamination. However, if stress singularities are present, a fracture mechanics characterization of matrix dominated failures may be more appropriate.

REFERENCES

1. Tennyson, R.C., MacDonald, D., and Nanyaro, A.P., "Evaluation of Tensor Polynomial Criterion for Composite Materials," J. of Composite Materials, Vol.12, Jan. 1978, p.63.

2. Francis, P.H., Walrath, D.E., and Weed, D.N., "Investigation of First Ply Failure in Graphite/Epoxy Laminates Subjected to Biaxial Static and Fatigue Loadings", AFML TR-77-62, June, 1977.

3. Lagace,P.A., and Brewer,J.C., "Studies of Delamination Growth and Final Failure under Tensile Loading," ICCM VI, London, Vol.5, Proceedings, July 1987, pp.262-273.

4. Brewer,J.C., and Lagace,P.A., "Quadratic Stress Criterion for Initiation of Delamination," J. of Composite Materials, Vol.22, No.4, Dec. 1988, pp.1141-1155.

5. W. Weibull, "A statistical Theory of the Strength of Materials," Ing. Vetenskaps Akad. Handl., (Royal Swedish Institute Engineering Research Proceedings, NR151, 1939.

6. Rodini, B.T., and Eisenmann, "An Analytical and Experimental Investigation of Edge Delamination in Composite Laminates," in Fibrous Composites in Structural Design, Plenum Publishers, New York, 1980, pp.441-457.

7. Adams, D.F., King, T.R., and Blackketter, D.M., "Evaluation of the Transverse Flexure Test Method for Composite Materials," Composites Science and Technology, Vol. 39, 1990, pp.341-353.

8. Crews, J.H.,Jr., and Naik, R.A., "Measurement of Multiaxial Ply Strength by an Off-axis Flexure Test," Presented at the ASTM 11th Conference on Composite Materials: Testing and Design, Pittsburgh, PA, May, 1992. (Also in NASA TM 10757, March, 1992.)

9. Kan, H.P., Bhatia, N.M., and Mahler, M.A., "Effect of Porosity on Flange-Web Corner Strength," in Composite Materials: Fatigue and Fracture, Third Vol., ASTM STP 1110, Sept. 1991, p.126.

10. Heil, C.C., Sumich, M., and Chappell, D.P., "A curved Beam Test Specimen for Determining the Interlaminar Tensile Strength of a Laminated Composite," J. of Composite Materials, Vol.25, July, 1991, p.854.

11. Jackson, W.C. and Martin, R.H., "An Interlaminar Tension Strength Specimen," Presented at the ASTM 11th Conference on Composite Materials: Testing and Design, Pittsburgh, PA, May, 1992.

12. Flaggs, D.L., and Kural, M.H., "Experimental Determination of the In Situ Transverse Lamina Strength in Graphite/Epoxy Laminates," J. of Composite Materials, Vol.16, March, 1982, p.103-116.

13. O'Brien, T.K. and Hooper, S.J., "Local Delamination in Laminates with Angle Ply Matrix Cracks: Part I, Tension Tests and Stress Analysis," NASA TM 104055, June, 1991 (Presented at the ASTM 4th Conference on Composite Materials: Fatigue and Fracture, Indianapolis, IN, May, 1991.

APPENDIX

Influence of Sample Size on Determination of Weibull Parameters

The accuracy of the two parameters, m and σ_c, obtained from the least squares regression fit of the logarithmic eq(3) may depend on the sample size, i.e., on the number of tests conducted. For example, table 9 lists the strength data for the 4,8,16,32 and 64-ply laminates in ascending order with their associated median rank corresponding to a probability of failure, $P(\sigma)$. This set of 33 data points yields a shape parameter, m, of 7.63 and a characteristic strength of 8.87 ksi. If these 33 tests were considered to be the total population, then any subset of these data would represent a sample based on a smaller number of tests performed to characterize the entire population.

Figures 30 and 31 show the apparent characteristic strength and shape parameter, respectively, for sample sizes of n = 5, 8, 16, and 21 tests representing four subsets of the data shown in table 9. The four subsets chosen were: (1) a subset using only the highest n

strength values (high n), (2) a subset using only the lowest n strength values (low n), (3) a subset using the intermediate n strength values (middle n), and (4) a subset using roughly equal numbers of data points from the highest and lowest ends of the total population (high/low n).

Subsets 1 and 2 represent upper and lower bounds on characteristic strength for a given sample size. For example, fig. 30 indicates that the variation in characteristic strength increases with decreasing sample size. Subset 4 typically represents an upper bound in terms of scatter (lower bound in value of m) whereas subsets 1 or 3 represent a lower bound in terms of scatter (upper bound in value of m). For example, fig. 31 indicates that the variation in the shape parameter increases dramatically with decreasing sample size.

Because the Weibull shape parameter, m, characterizes the extent of scatter inherent in the ultimate strength measurement, a large number of tests are required to determine m accurately for a given material system. Ideally, a large number of tests will be conducted on a single configuration to obtain the Weibull parameters. In this case, the accuracy of the shape parameter, m, depends primarily on how well the total sample approximates the population to be characterized. However, because only 3-4 replicates were tested for each unique configuration in this study, a unique value of m could not be accurately determined for each combination of specimen width and thickness. However, for the reasons cited in the text, all the measured strengths from all the 90 degree tests conducted in this study were combined to estimate m.

TABLE 1

Nominal Ply Thickness and Fiber Volume Fraction
90 degree tension tests
AS4/3501-6 Graphite Epoxy

	4 ply	8 ply	16 ply	32 ply	64 ply
Ply Thickness, h, in.	0.0048	0.0046	0.0046	0.0048	0.0050
V_f, %	68%	71%	71%	68%	66%

TABLE 2

Failure Loads in lbs for 90 degree tension tests
AS4/3501-6 Graphite Epoxy

width, in.	4 ply	8 ply	16 ply	32 ply	64 ply
0.5	96 72* 90*	186 188 176	278 304 #	700 570* 564	1287 1182 1199 1121
1.0	150 162 166	373 400 384	625 523 643	1140 938 1439	2109 2052* 1937*
2.0	264* 317 #	640* 490* 589*	1293 1125 1388	2283 2185 2211	4450

* Grip Failure
\# Accidental Failure

TABLE 3

Nominal Transverse Tensile Strength in ksi from
90 degree tension tests
AS4/3501-6 Graphite Epoxy

width, in.	4 ply	8 ply	16 ply	32 ply	64 ply
0.5	9.75	10.12	7.48	9.56	8.11
	*	10.03	8.16	*	7.47
	*	9.45		7.13	7.34
					7.08
1.0	7.79	10.27	8.49	7.38	6.45
	8.38	10.90	7.03	6.01	*
	8.60	10.39	8.70	9.39	*
2.0	*	*	8.88	7.58	7.08
	8.23	*	7.70	7.02	
		*	9.71	7.50	

* Grip Failure

TABLE 4

Local Transverse Tensile Strength in ksi from
90 degree tension tests
AS4/3501-6 Graphite Epoxy

width, in.	4 ply	8 ply	16 ply	32 ply	64 ply
0.5	#	#	7.56	9.65	8.16
	*	#	8.36	*	7.51
	*	9.21		7.30	7.41
					7.05
1.0	7.76	10.86	8.54	7.46	6.58
	8.69	#	7.35	6.01	*
	8.83	10.69	9.07	9.57	*
2.0	*	*	8.96	7.96	7.25
	8.98	*	7.70	7.23	
		*	9.84	7.86	

* Grip Failure
# Failed in more than one location

TABLE 5

Transverse Tensile Failure Strain in με from 0.062 inch gage
90 degree tension tests
AS4/3501-6 Graphite Epoxy

width, in.	4 ply	8 ply	16 ply	32 ply	64 ply
0.5	5910	#	5070	#	
	*	#	4840	*	
	*	5970		4770	
1.0	#	#	5490	#	
	6620	6880	4750	4080	
	5500	6220	5100	6600	
2.0	*	*	#	#	
	6360	*	5400	4980	
		*	5520	4650	

* Grip Failure
\# 0.062 in. gage not mounted on specimen

TABLE 6

Transverse Tensile Failure Strain in με from 0.125 inch gage
90 degree tension tests
AS4/3501-6 Graphite Epoxy

width, in.	4 ply	8 ply	16 ply	32 ply	64 ply
0.5	#	6170	4300	6090	5365
	*	6120	5280	*	5315
	*	5920		5000	5130
					5205
1.0	#	6500	#	5140	4365
	4720	6280	4270	3810	*
	6180	6800	6800	6560	*
2.0	*	*	5620	5200	6140
	4760	*	4410	4620	
		*	6450	5220	

* Grip Failure
\# 0.125 in. gage not mounted on specimen

TABLE 7

Transverse Tensile Failure Strain in με from 1.0 inch extensometer
90 degree tension tests
AS4/3501-6 Graphite Epoxy

width, in.	4 ply	8 ply	16 ply	32 ply	64 ply
0.5			5020 5500	# * 4810	
1.0			5610 4620 6180	# 4060 6250	
2.0			5810 4900 6160	# 4820 4760	

* Grip Failure
\# 1.0 in. extensometer not mounted on specimen

TABLE 8

Average Transverse Tensile Failure Strain in με
16 & 32-ply 90 degree tension tests (n=11)

	0.062 inch gage	0.125 inch gage	1.0 in. clip gage	AVG	CV,%
mean	5069	5156	5190	5138	1.2%
C.V., %	13%	20%	14%		

TABLE 9

Median Ranking of Nominal Transverse Strength
4, 8, 16 &32-ply 90 degree tension tests
AS4/3501-6 Graphite Epoxy

i	Strength, ksi	P(σ)
1	6.010	0.026
2	7.020#	0.062
3	7.030	0.099
4	7.130#	0.135
5	7.380	0.172
6	7.480	0.208
7	7.500	0.245
8	7.580	0.281
9	7.700	0.318
10	7.790@	0.354
11	8.160	0.391
12	8.230@	0.427
13	8.380@	0.464
14	8.490	0.500
15	8.600@	0.536
16	8.700	0.573
17	8.880	0.609
18	9.390	0.646
19	9.450	0.682
20	9.560#	0.719
21	9.710	0.755
22	9.750@	0.738
23	10.030	0.828
24	10.120	0.865
25	10.270	0.901
26	10.390	0.938
27	10.900	0.974

\# Near-grip failures within 0.1w from grip line
@ 4-ply laminates

TABLE 10

Average measured volumes in cubic inches
for 90 degree tension tests
AS4/3501-6 Graphite Epoxy

width, in.	4 ply	8 ply	16 ply	32 ply	64 ply
0.5	.070 B	.133 C	.259 D	.511 E	1.12 F
1.0	.133 C	.259 D	.518 E	1.08 F	2.29 G
2.0	.261 D	.523 E	1.02 F	2.10 G	4.40 H

TABLE 11

Average Volumes and Strengths
for 90 degree tension tests
AS4/3501-6 Graphite Epoxy

Vol. Type	avg. Vol., in^3	avg. σ_{ult}, Ksi	low-high σ_{ult}, Ksi	no. tests, n	CV, %
A - small A - Large	0.000007 0.0334	11.97	9.53-15.5	5	20.3
B	0.07	9.75		1	
C	0.132	9.06	7.79-10.12	6	10.5
D	0.259	9.24	7.48-10.9	6	15.6
E	0.524	8.18	7.03-9.56	5	13.2
F	1.073	7.91	6.01-9.39	10	14.3
G	2.195	7.14	6.45-7.58	4	7.3
H	4.40	7.08		1	

Figure 1 **PANELS FOR 90 DEGREE TENSILE TESTS**

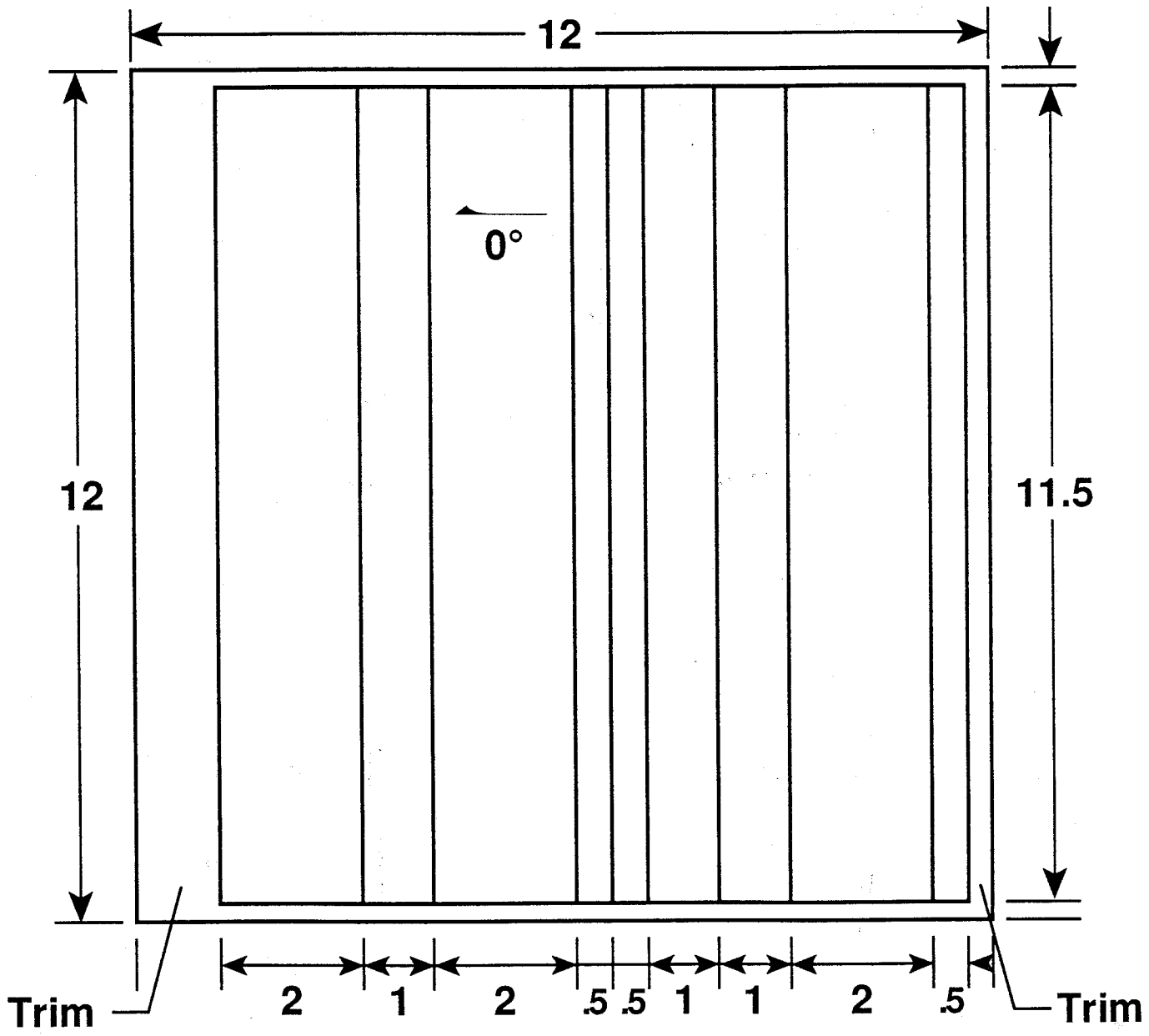

Figure 2 **STRAIN MEASUREMENT CONFIGURATIONS**

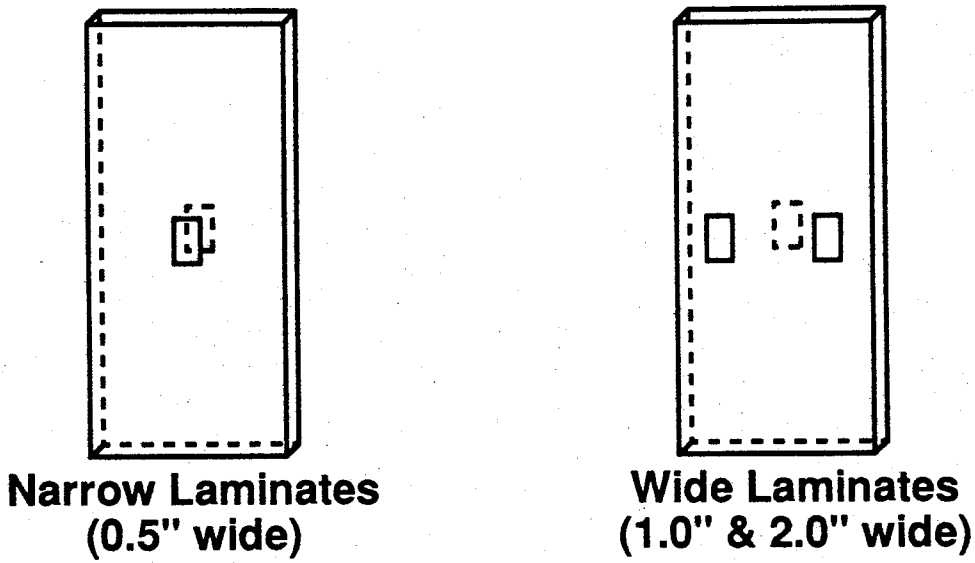

(a) Bending check configuration

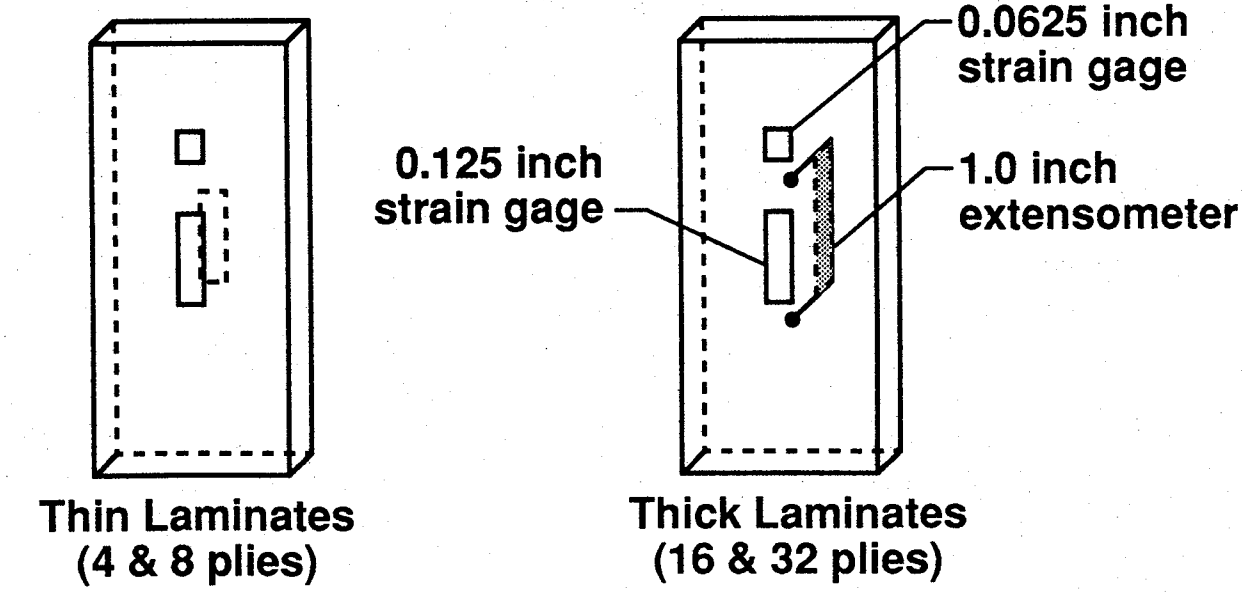

(b) Gage size effect configuration

Figure 3

TUNING FORK GRIP ARRANGEMENT

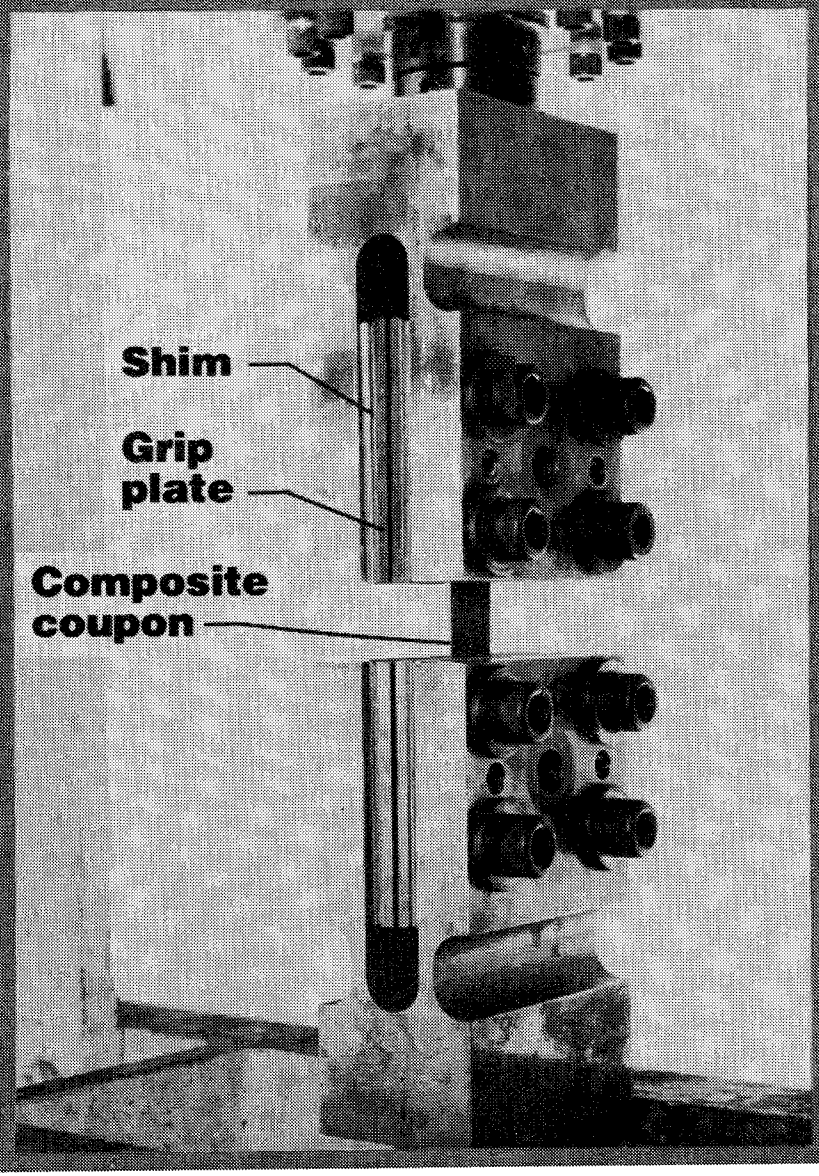

Figure 4 Transverse Tensile Strength of AS4/3501-6

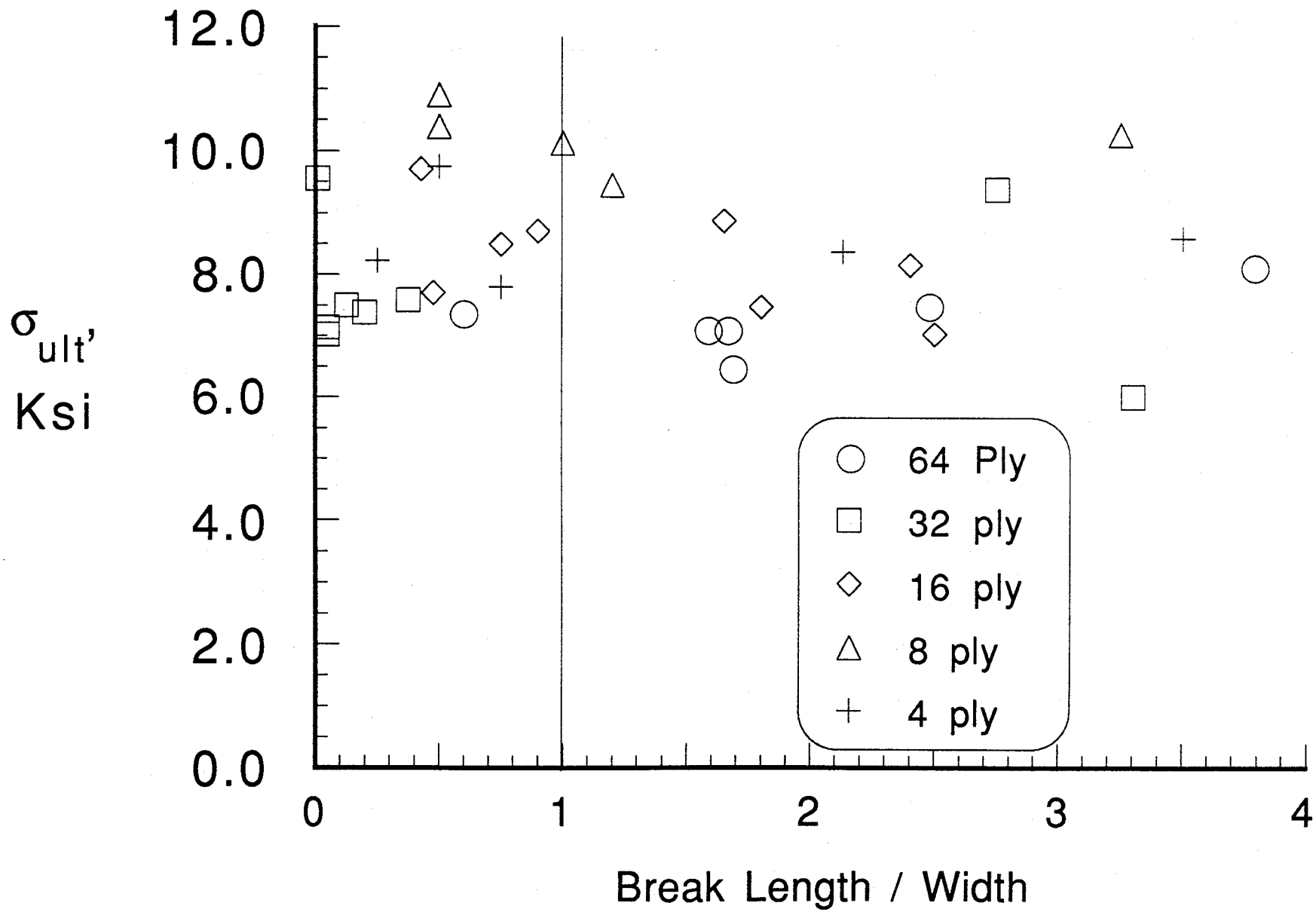

Figure 5 Transverse Tensile Strength of AS4/3501-6

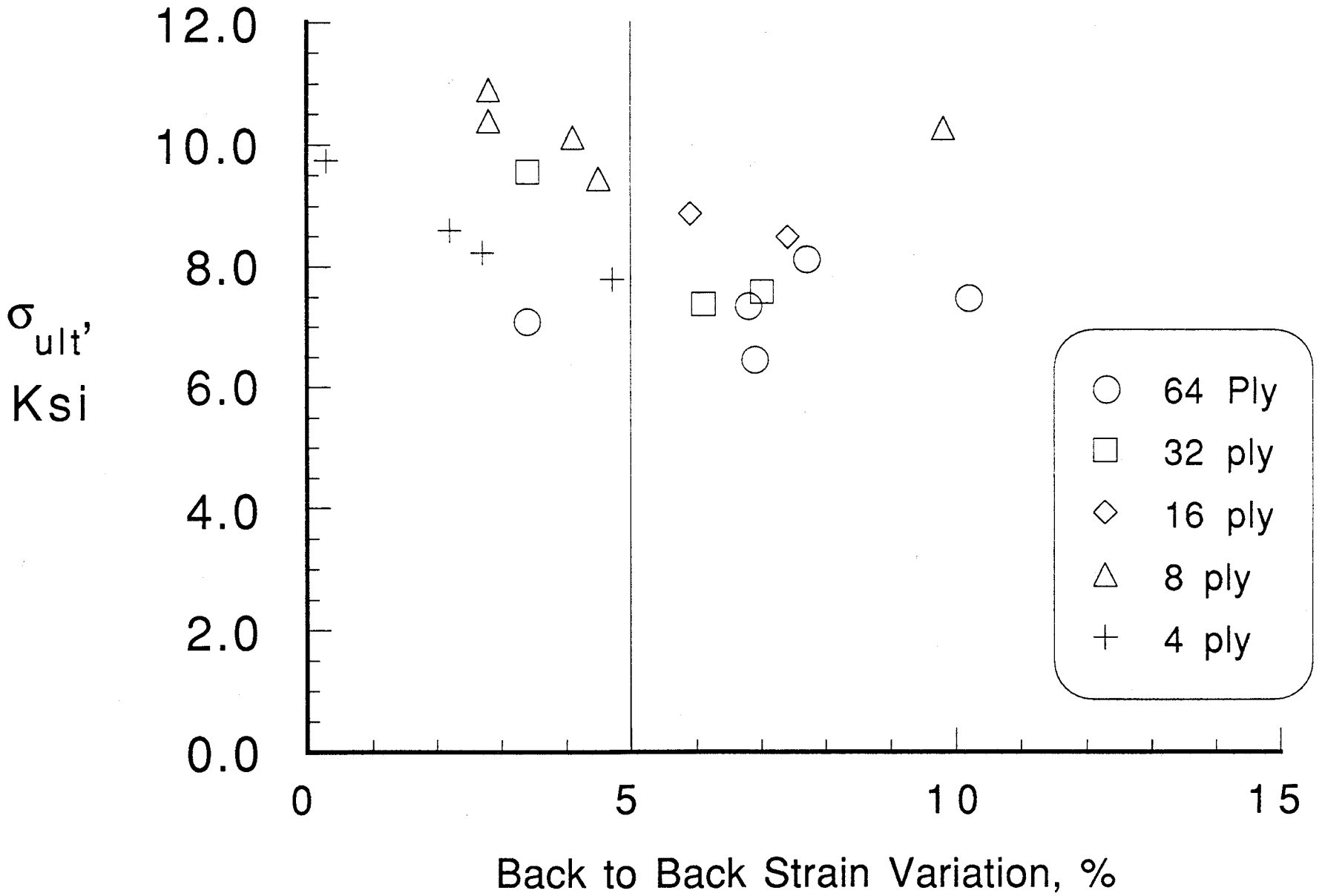

Figure 6 **LAMINATE CONFIGURATION AND LOADING FOR ANALYSIS**

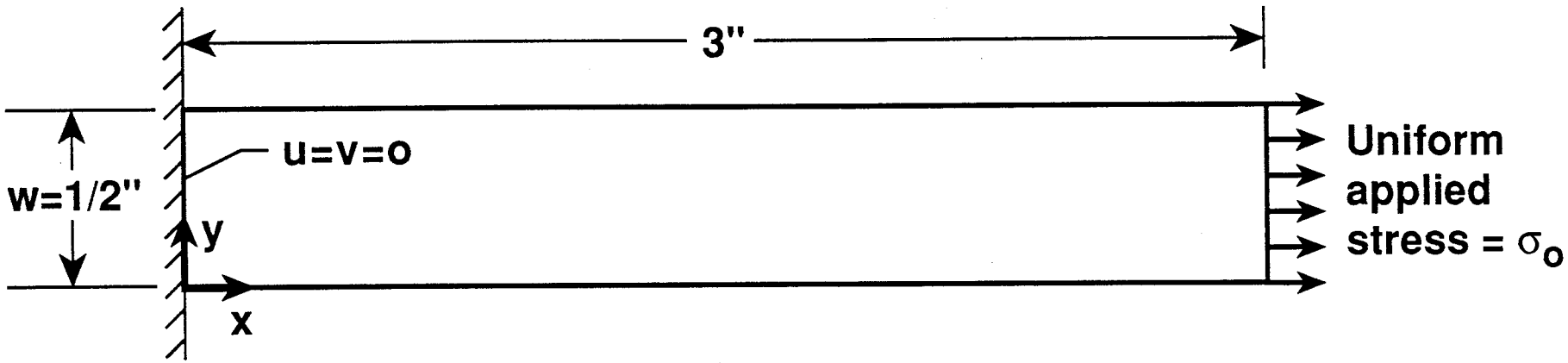

- Uniform finite element mesh
- Element size: .025" x .025"
- 7481 nodes, 2400 elements

Figure 7 **NORMALIZED TRANSVERSE STRESS DISTRIBUTION NEAR GRIP IN 90° LAMINATE**

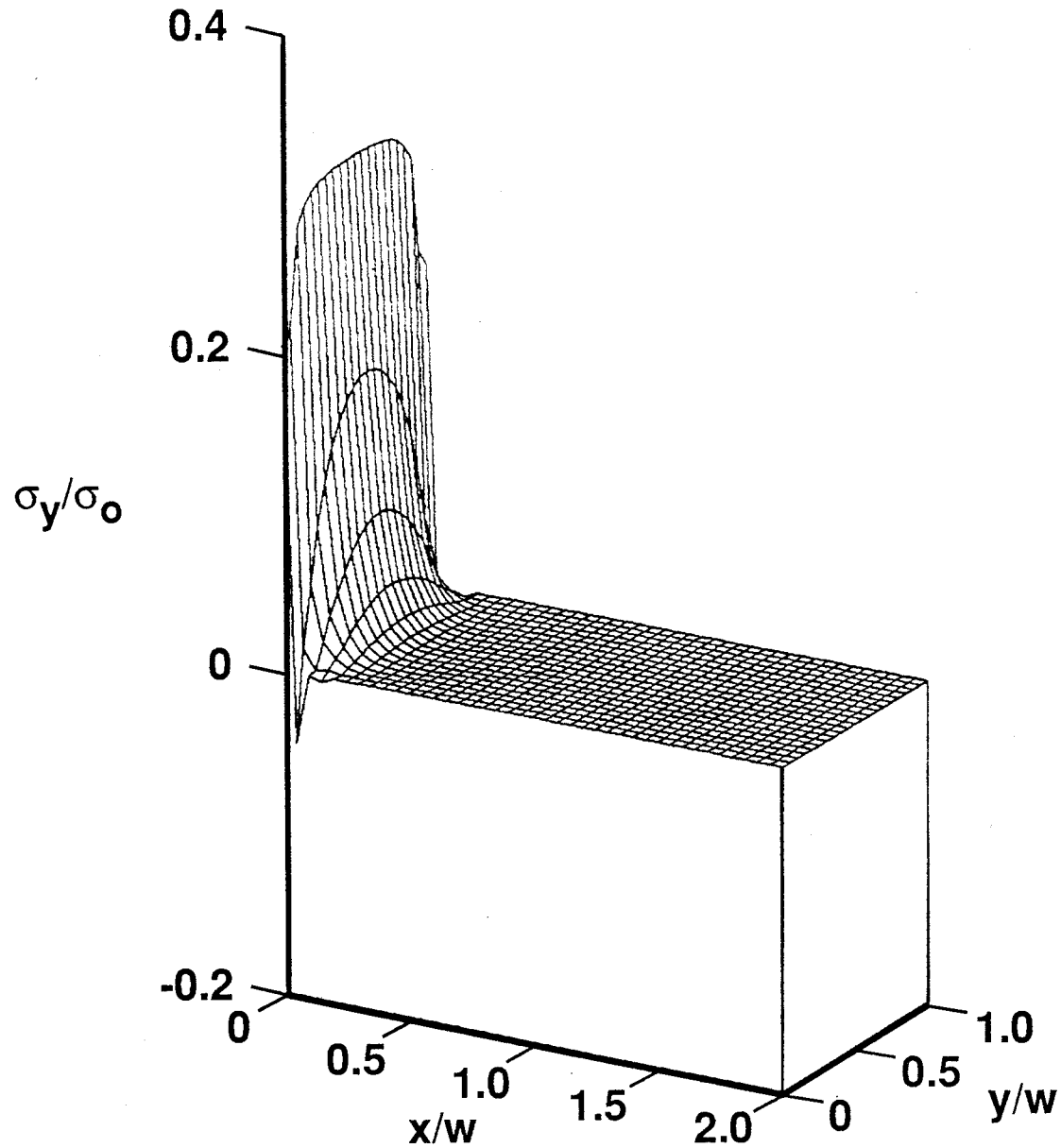

Figure 8 **COMPARISON OF NORMALIZED TRANSVERSE STRESS DISTRIBUTIONS NEAR GRIP FOR 0, 90, 0/90 AND QUASI-ISOTROPIC LAMINATES**

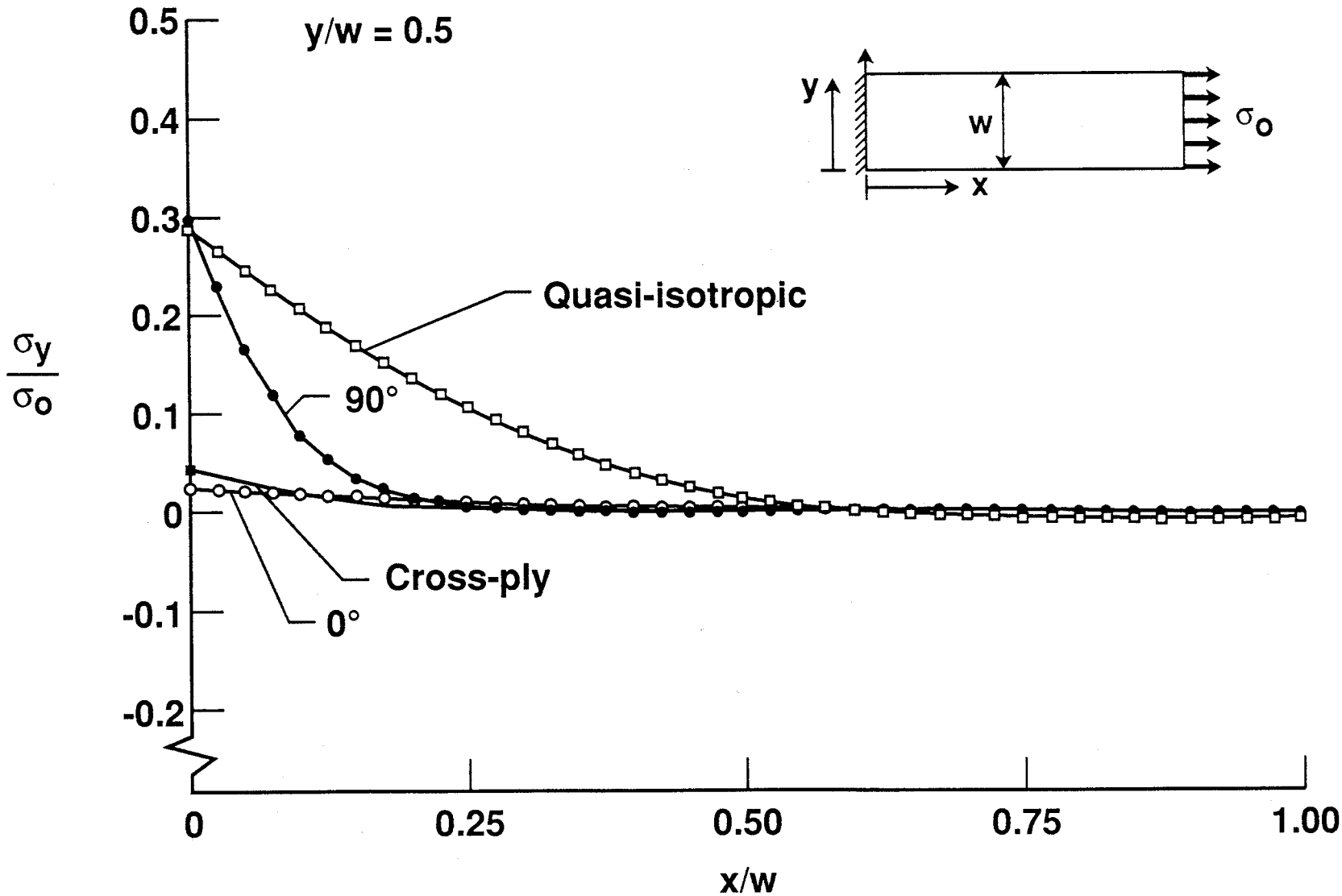

Figure 9 **NORMALIZED AXIAL STRESS DISTRIBUTION NEAR GRIP IN 90° LAMINATE**

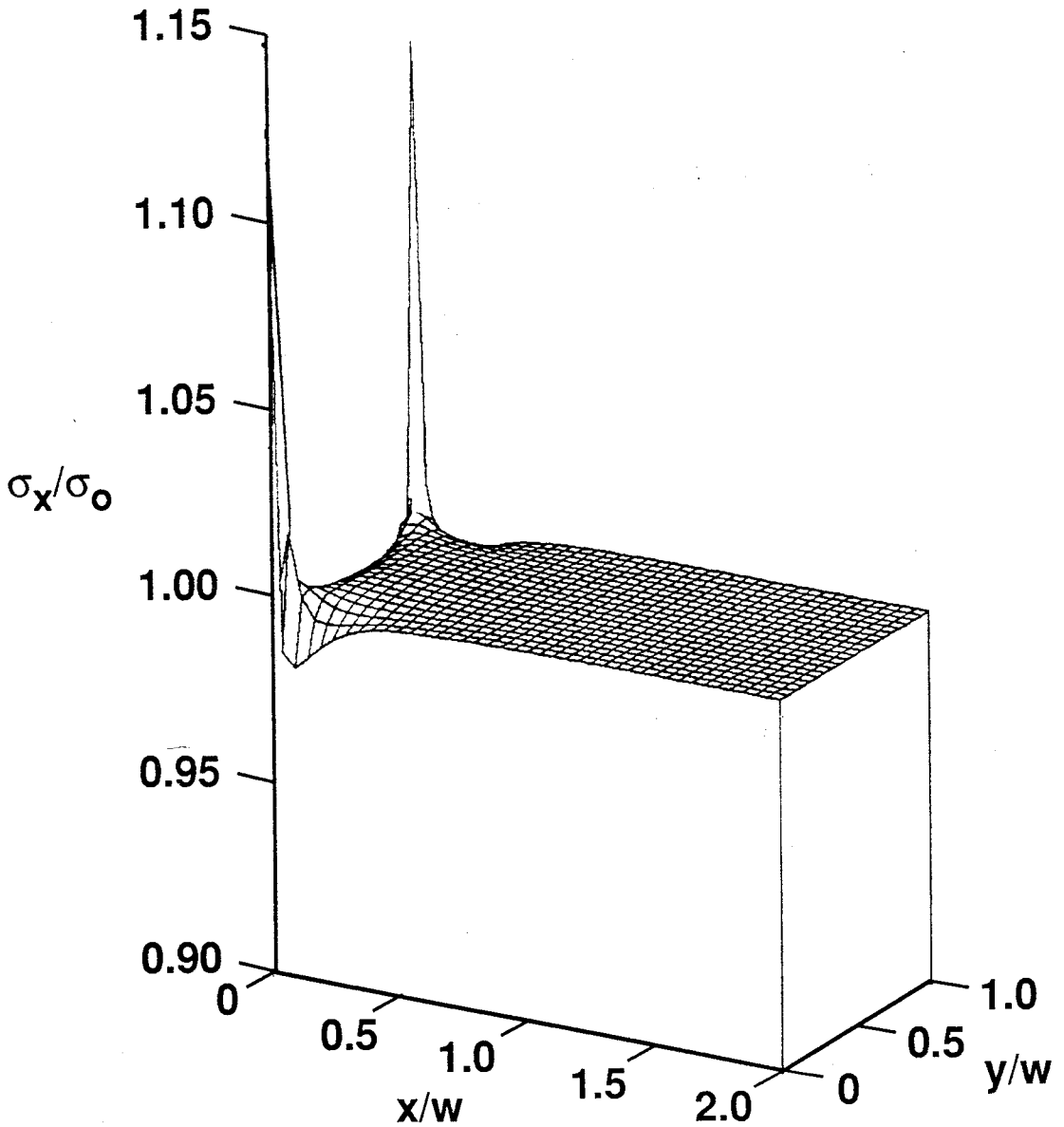

Figure 10 **NORMALIZED SHEAR STRESS DISTRIBUTION NEAR GRIP IN 90° LAMINATE**

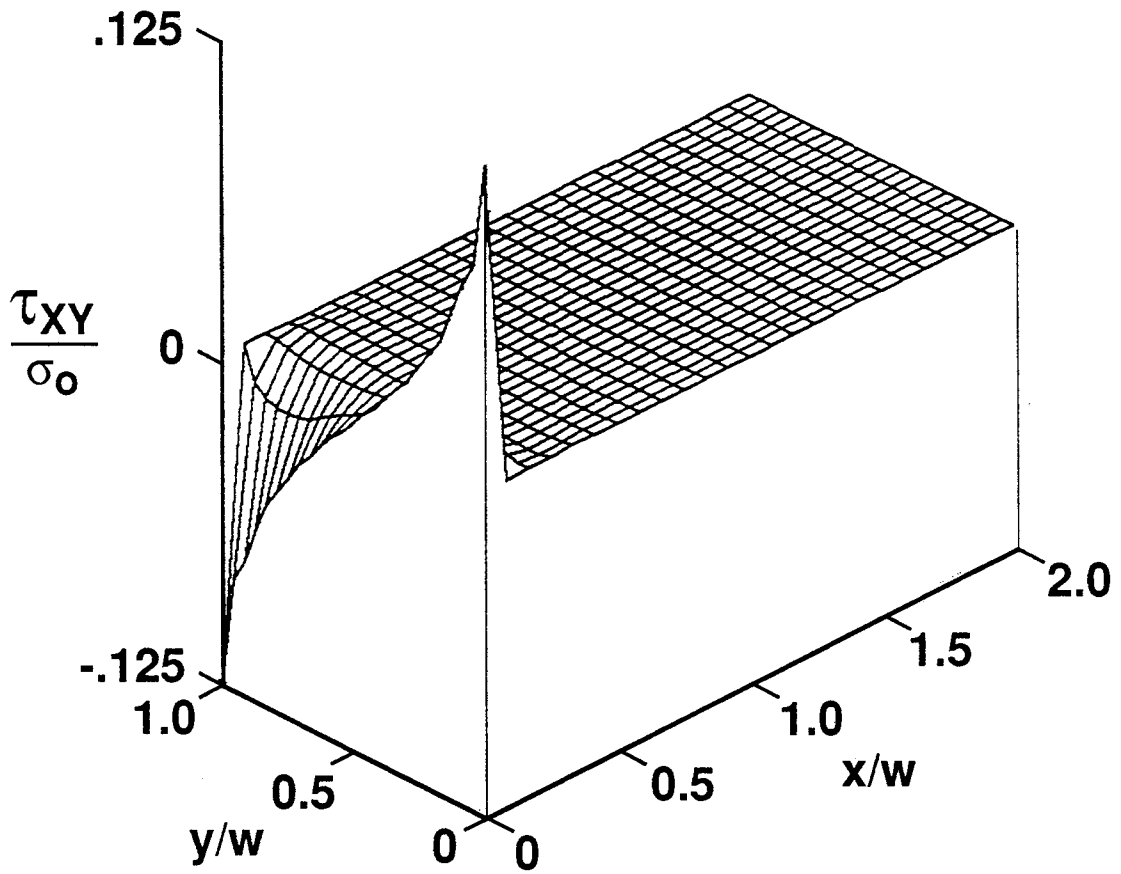

Figure 11 **COMPARISON OF NORMALIZED AXIAL STRESS DISTRIBUTIONS NEAR GRIP FOR 0° AND 90° LAMINATES**

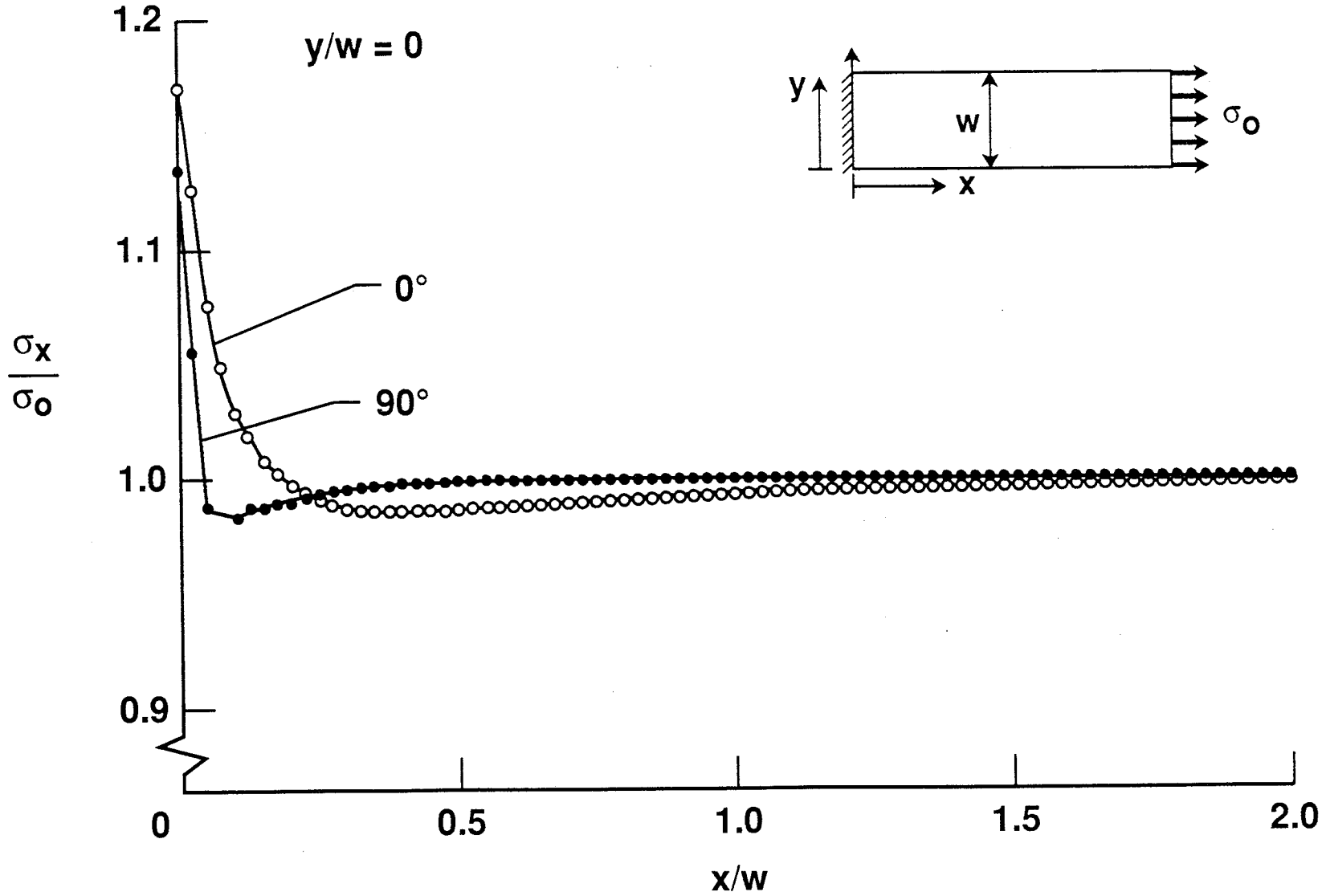

Figure 12 **COMPARISON OF NORMALIZED AXIAL STRESS DISTRIBUTIONS NEAR GRIP FOR 90°, 0/90 AND QUASI-ISOTROPIC LAMINATES**

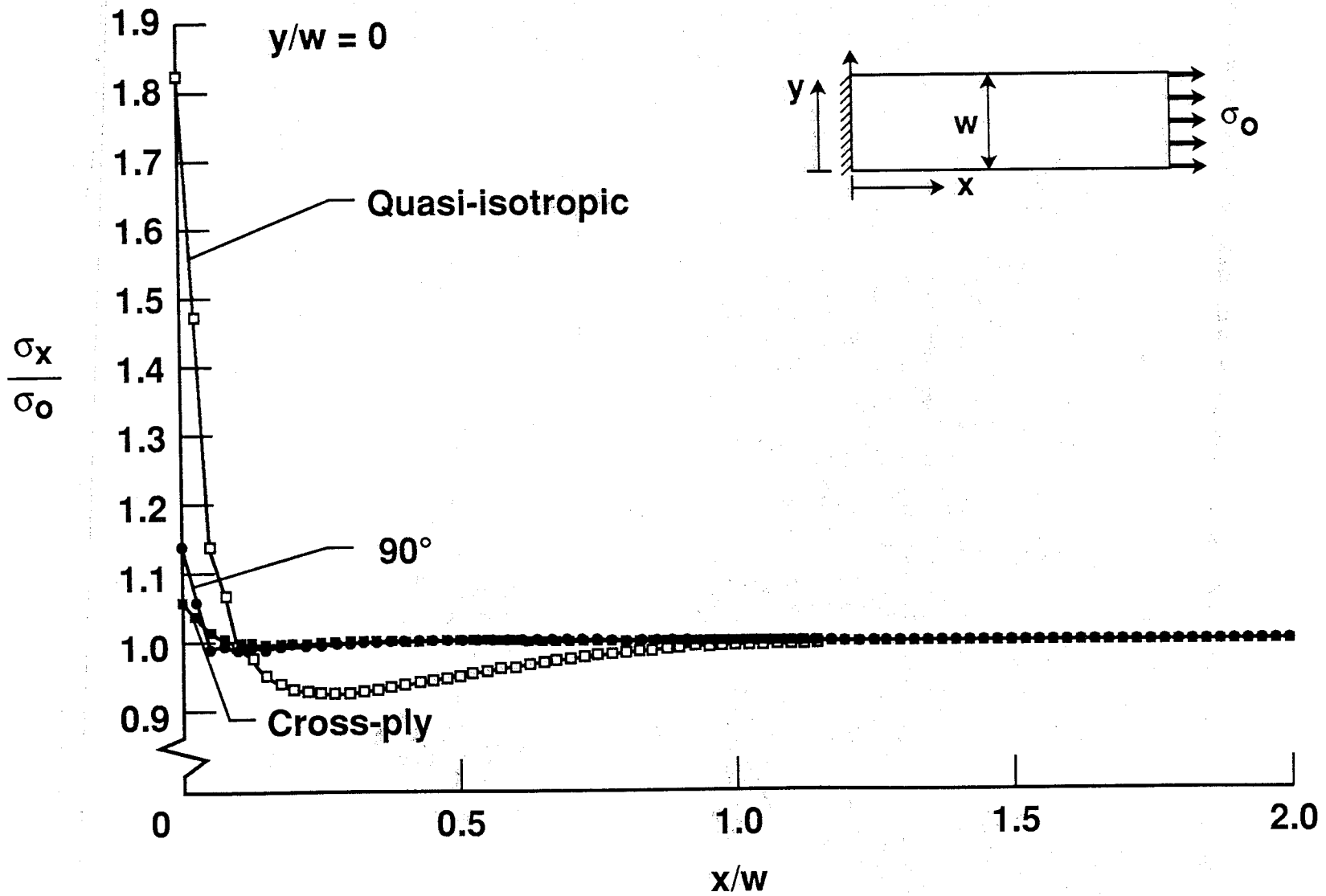

Figure 13 **NORMALIZED SHEAR STRESS DISTRIBUTION NEAR GRIP FOR 90° LAMINATE**

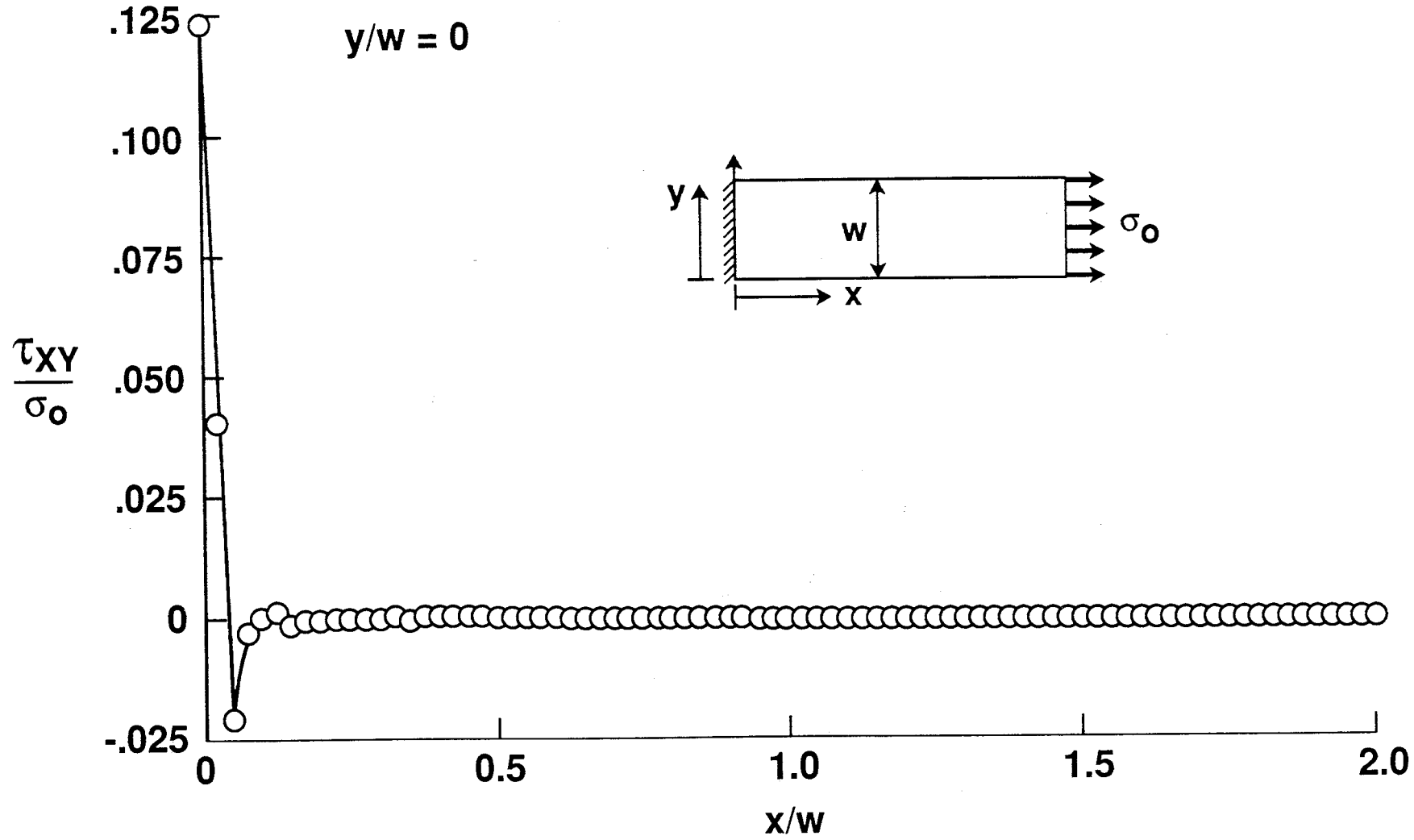

Figure 14 Transverse Tensile Strength of AS4/3501-6

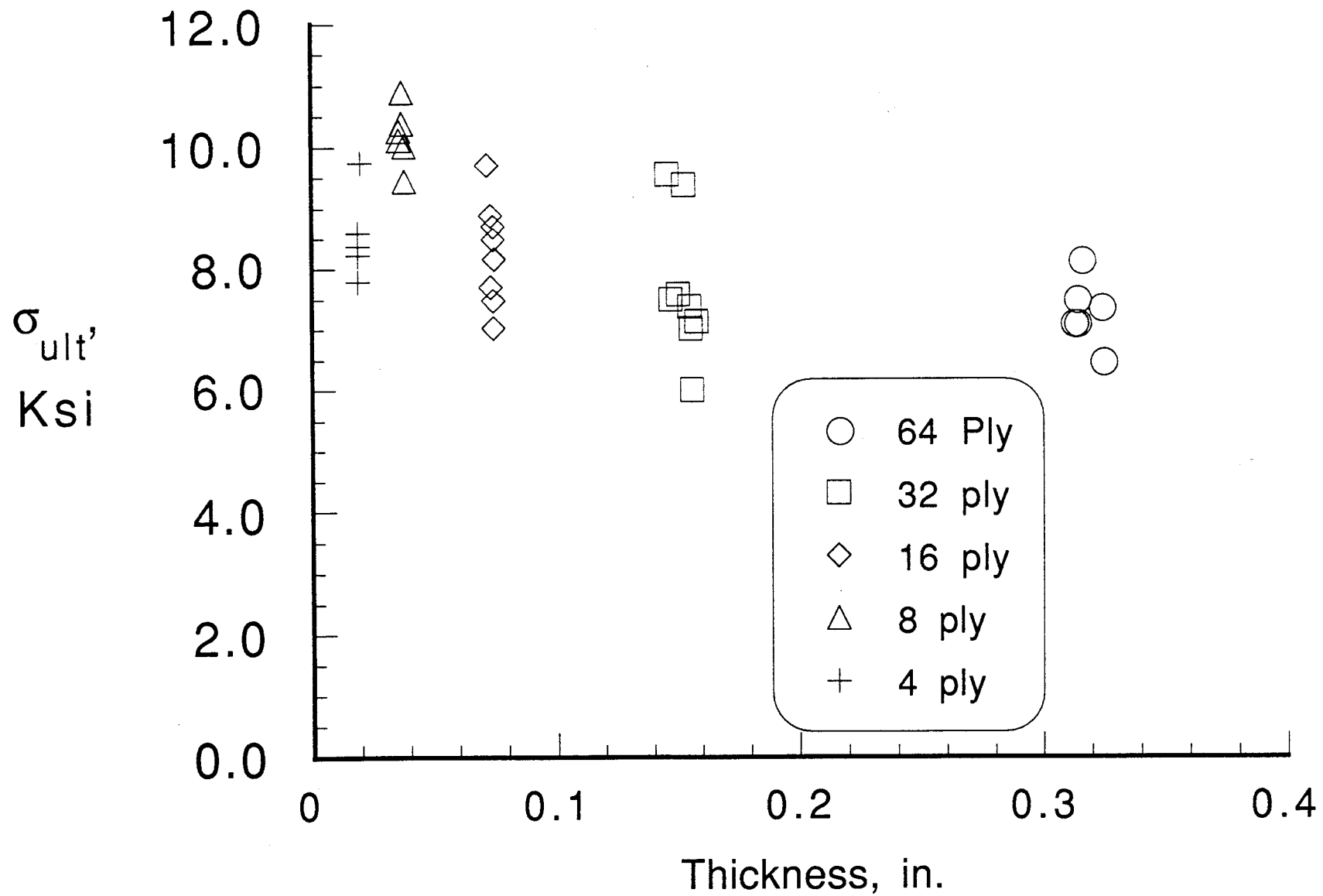

Figure 15 Transverse Tensile Strength of AS4/3501-6

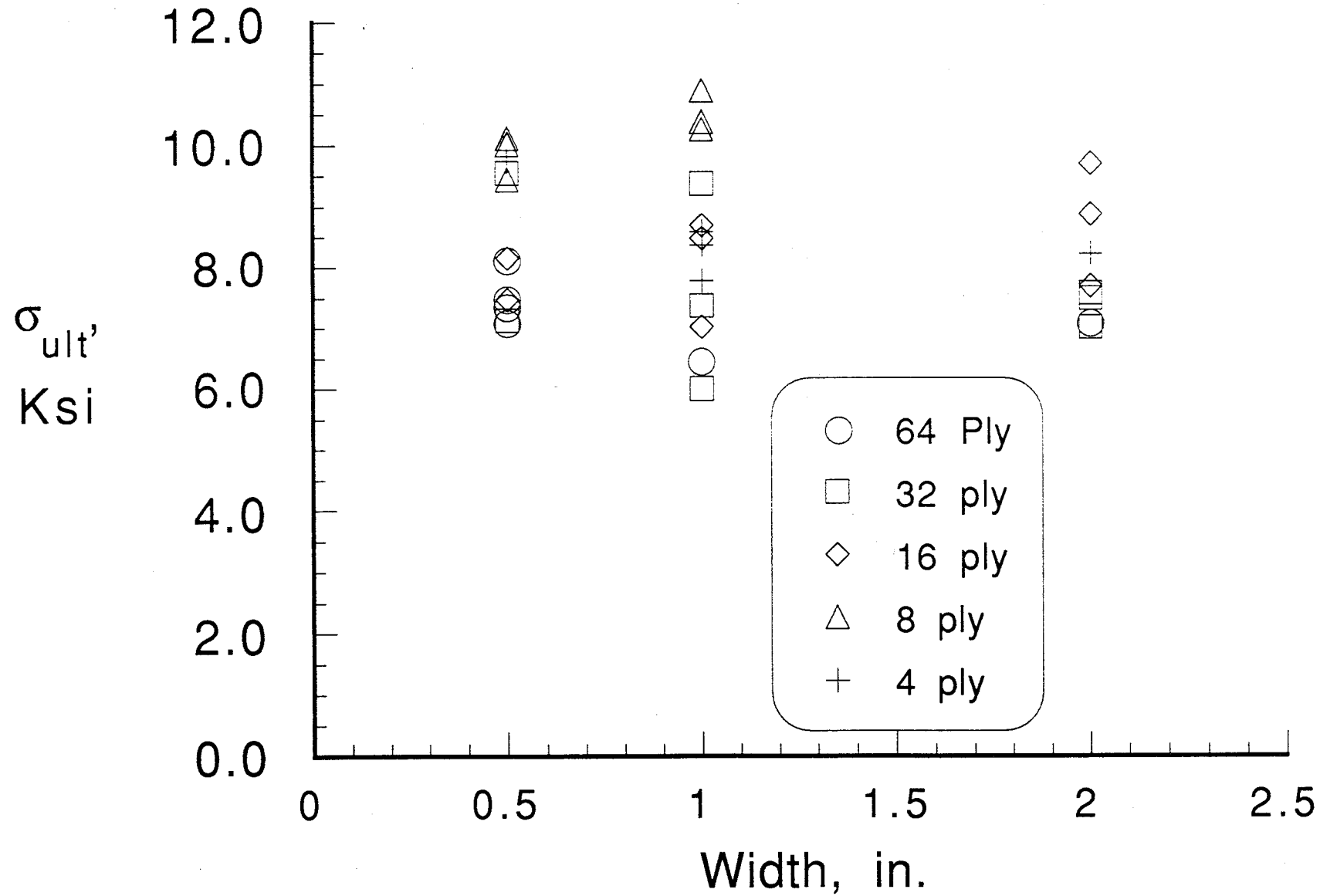

Figure 16 Transverse Tensile Strength of AS4/3501-6

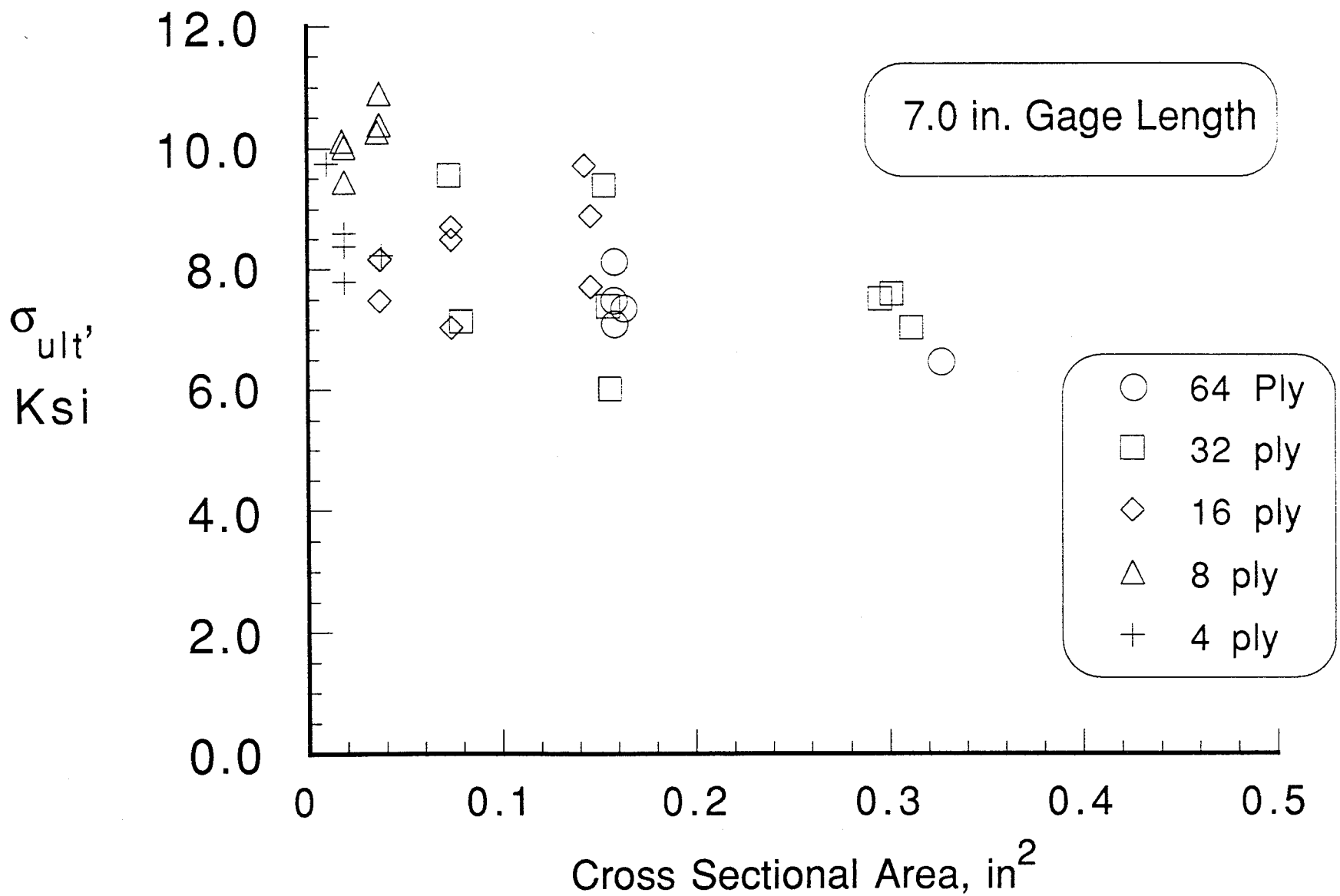

Figure 17 Transverse Tensile Strength Distribution

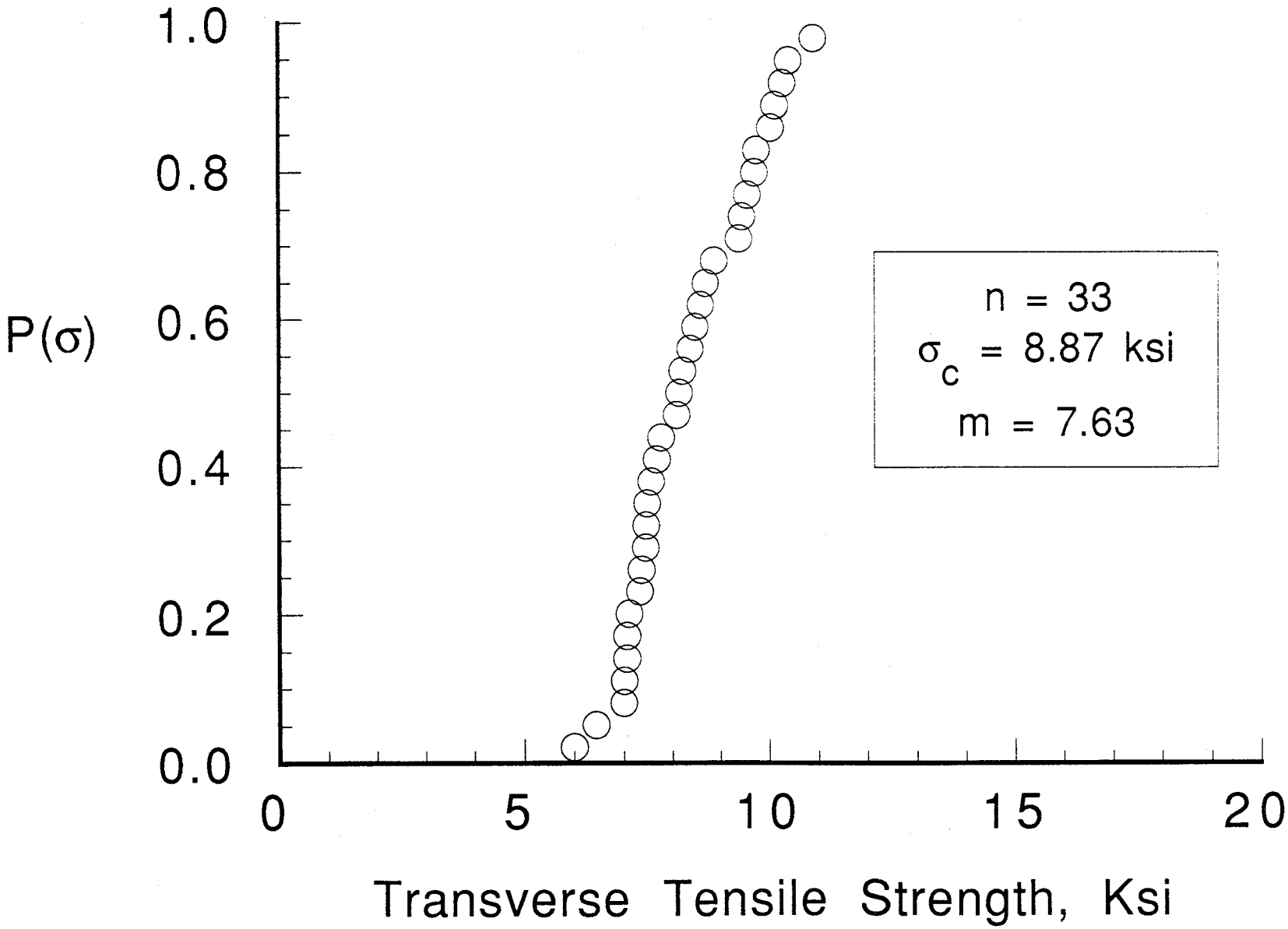

Figure 18 Transverse Tensile Strength Distribution

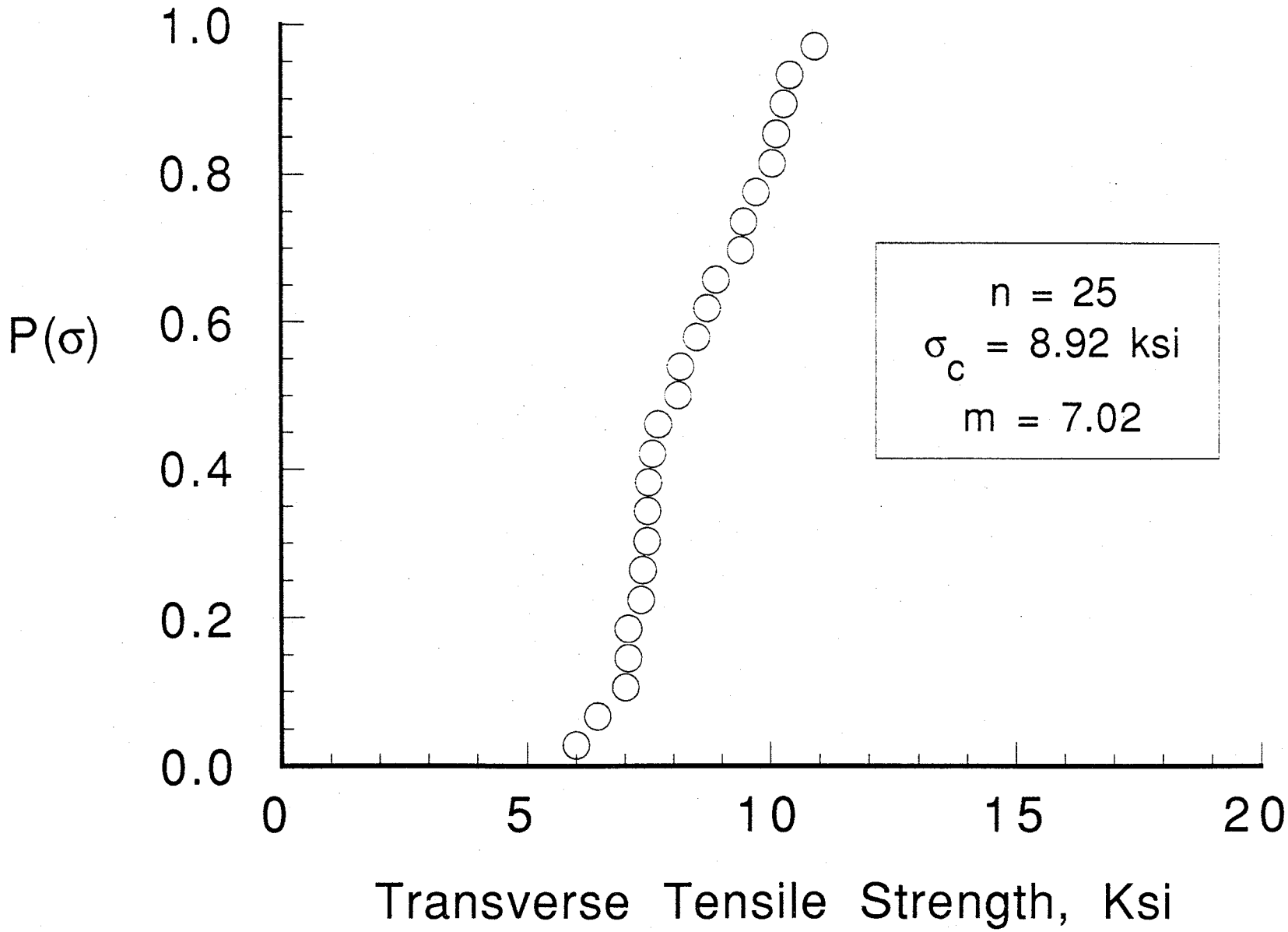

Figure 19 Transverse Tensile Strength of AS4/3501-6

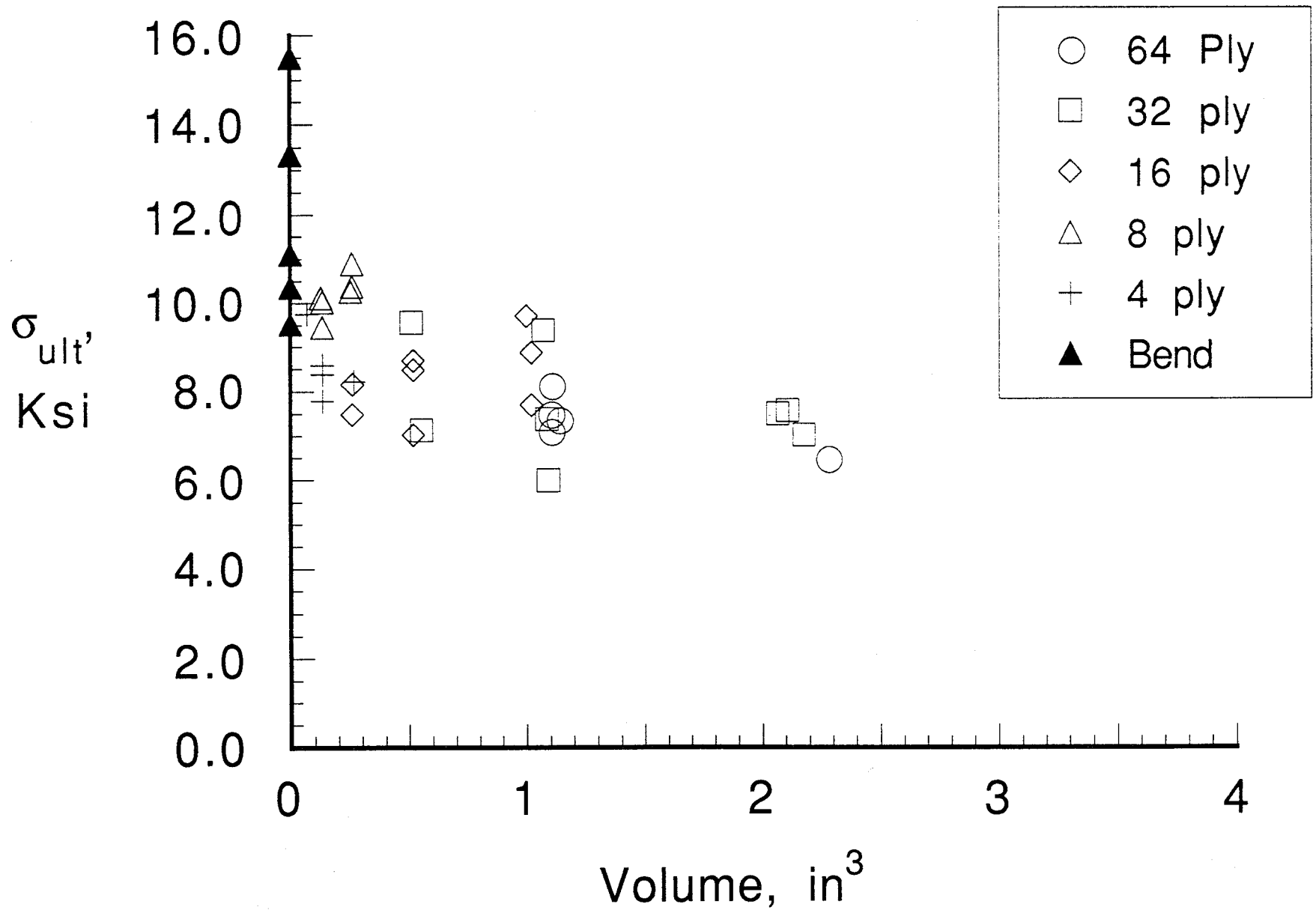

Figure 20 **LOCAL VOLUME IN THREE POINT BEND TESTS**

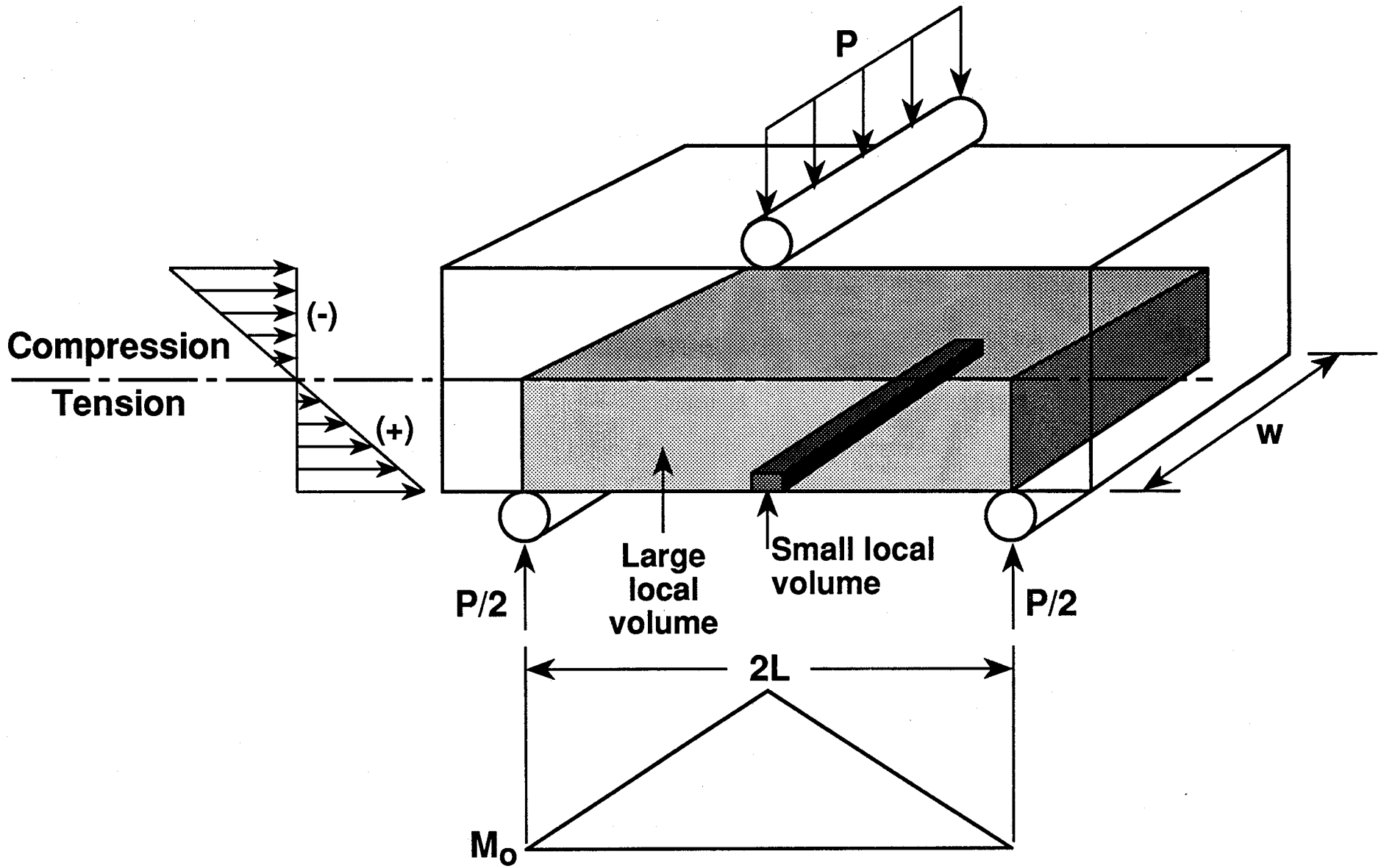

Figure 21 Predicted 90 Degree Flex Strength
Small Local Volume

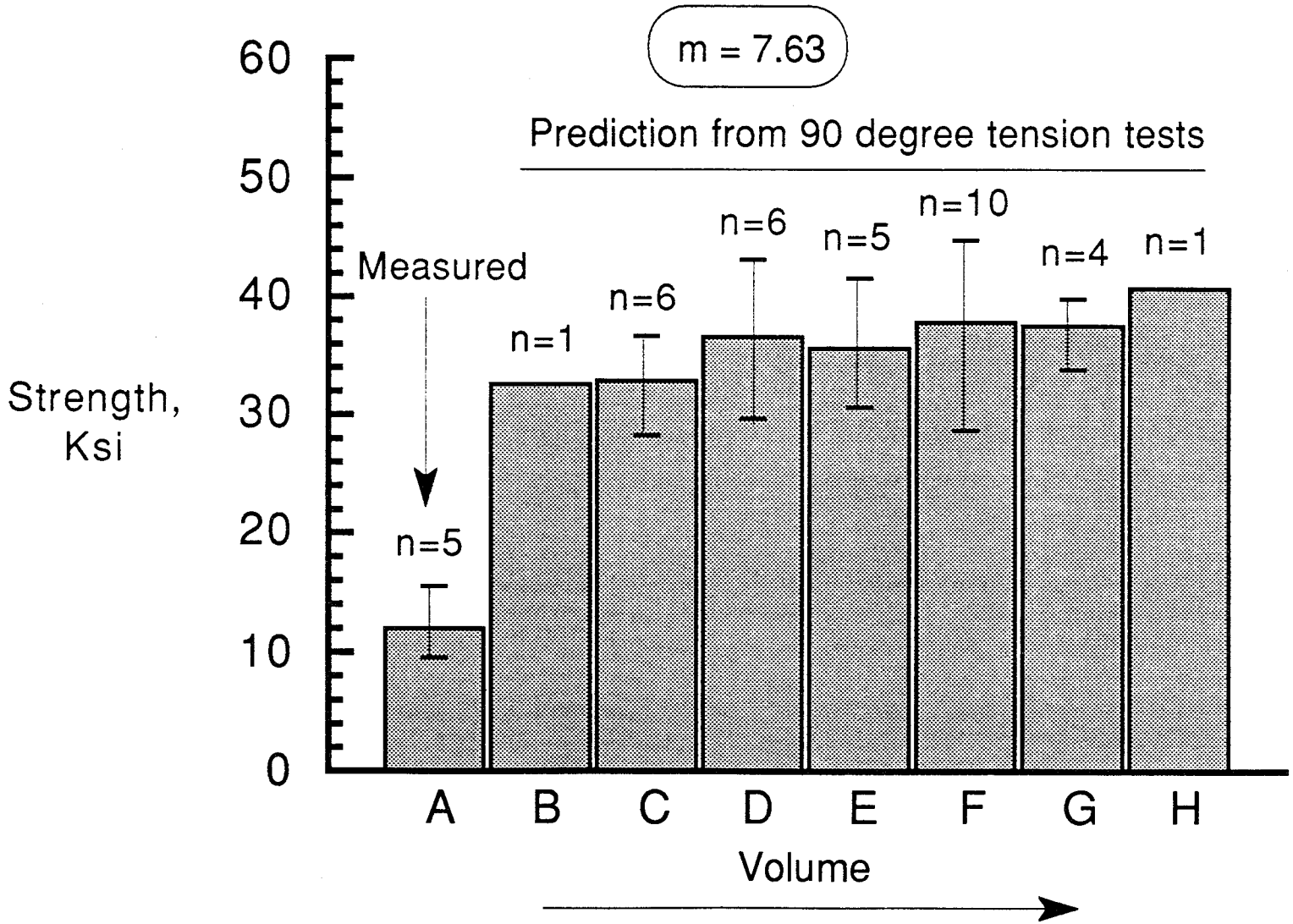

Figure 22 Predicted 90 Degree Flex Strength
Large Local Volume

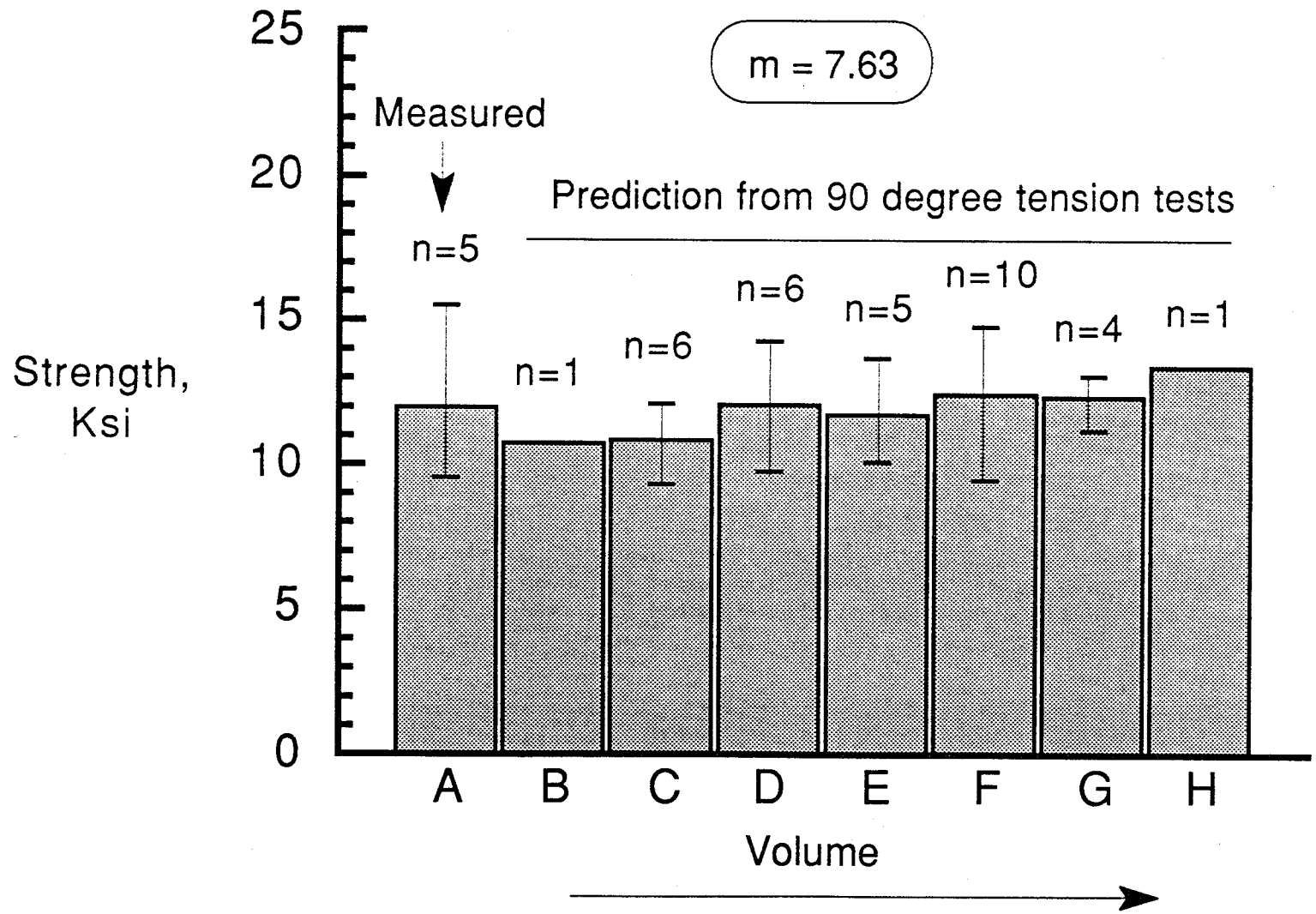

Figure 23 Predicted 90 Degree Flex Strength
Large Local Volume

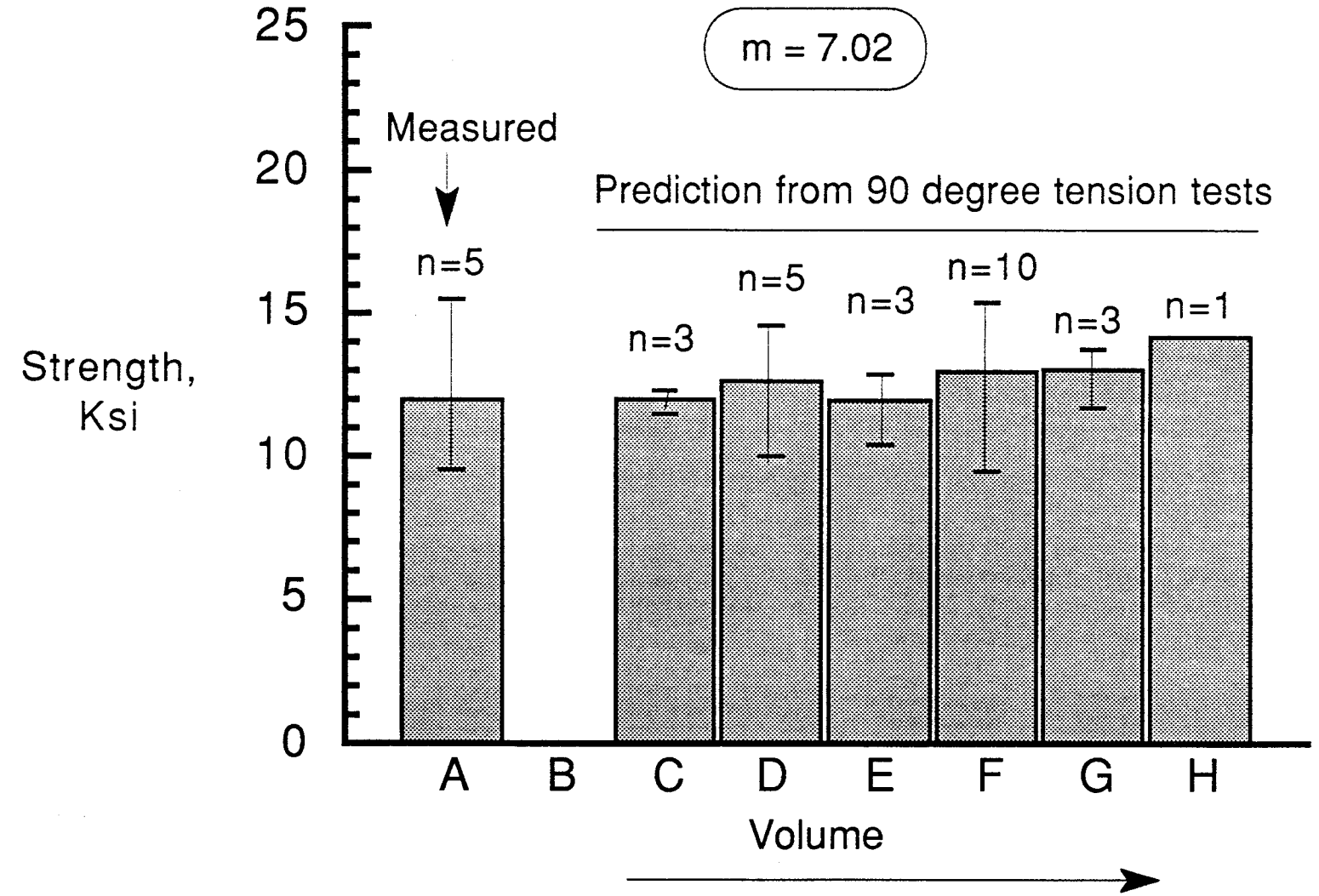

Figure 24 Transverse Tensile Strength of AS4/3501-6

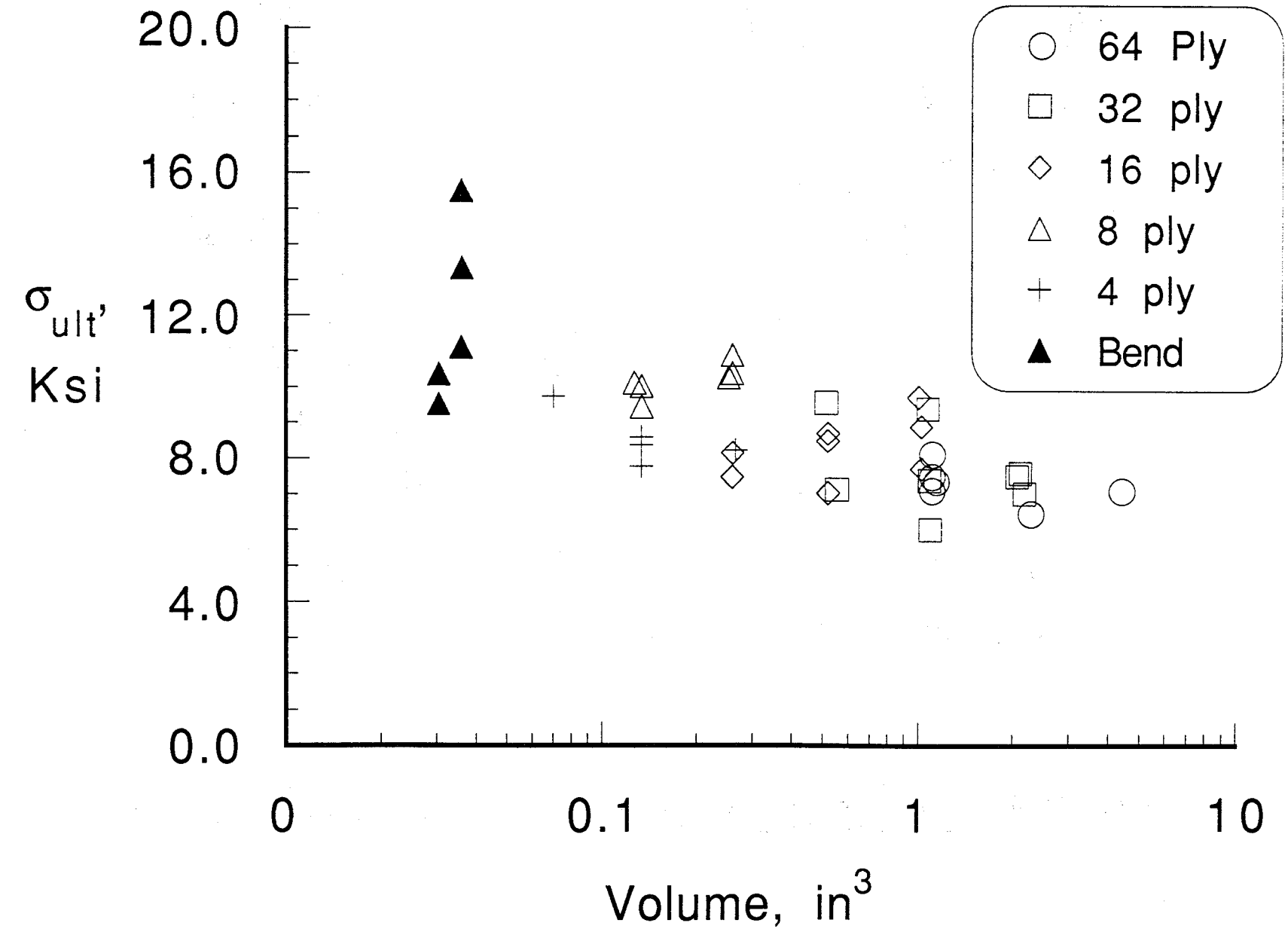

Figure 25 **LOCAL VOLUME IN CURVED BEAM TESTS**

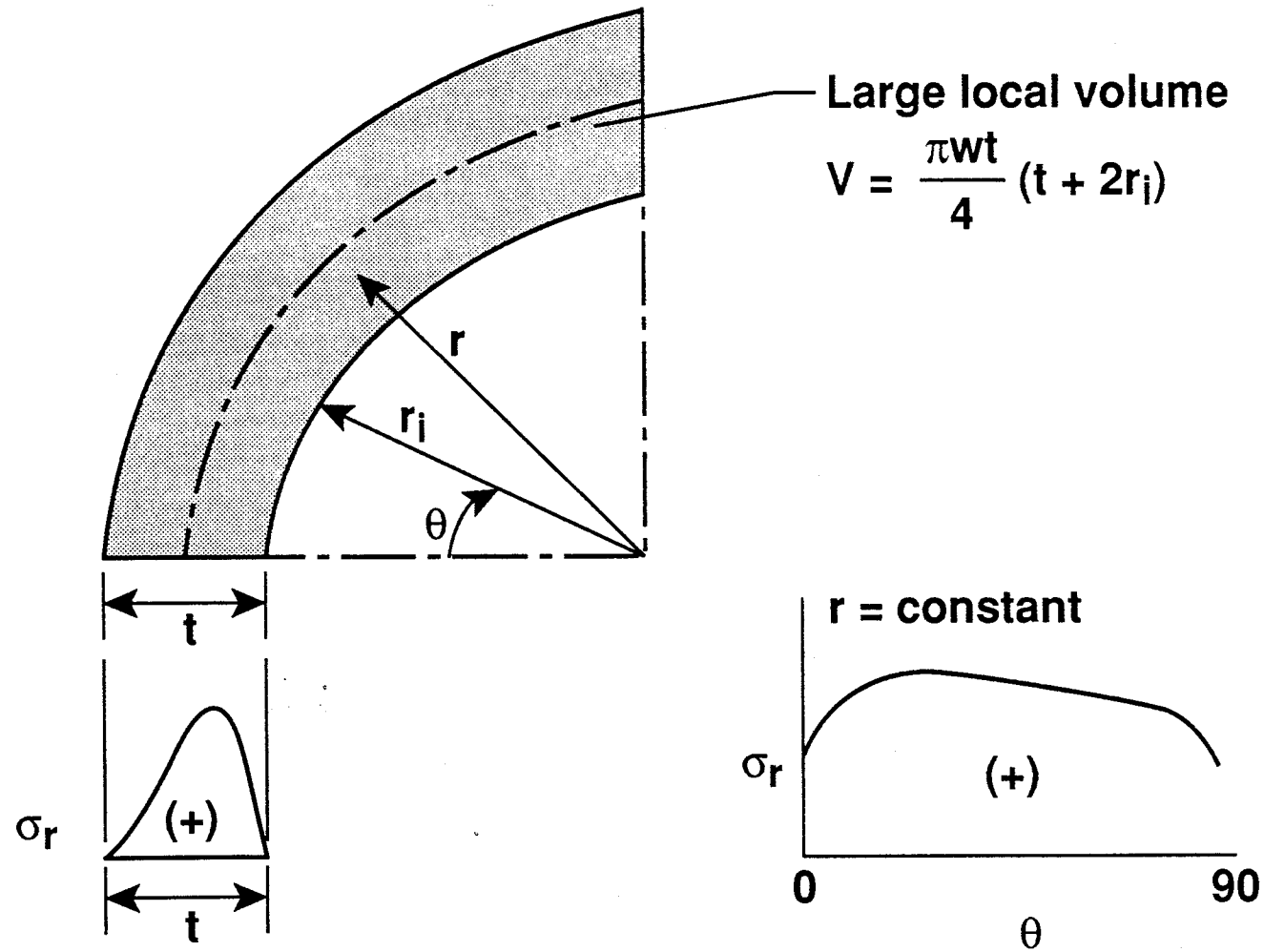

Figure 26 Curved Beam vs. Bend Test Strength of AS4/3501-6

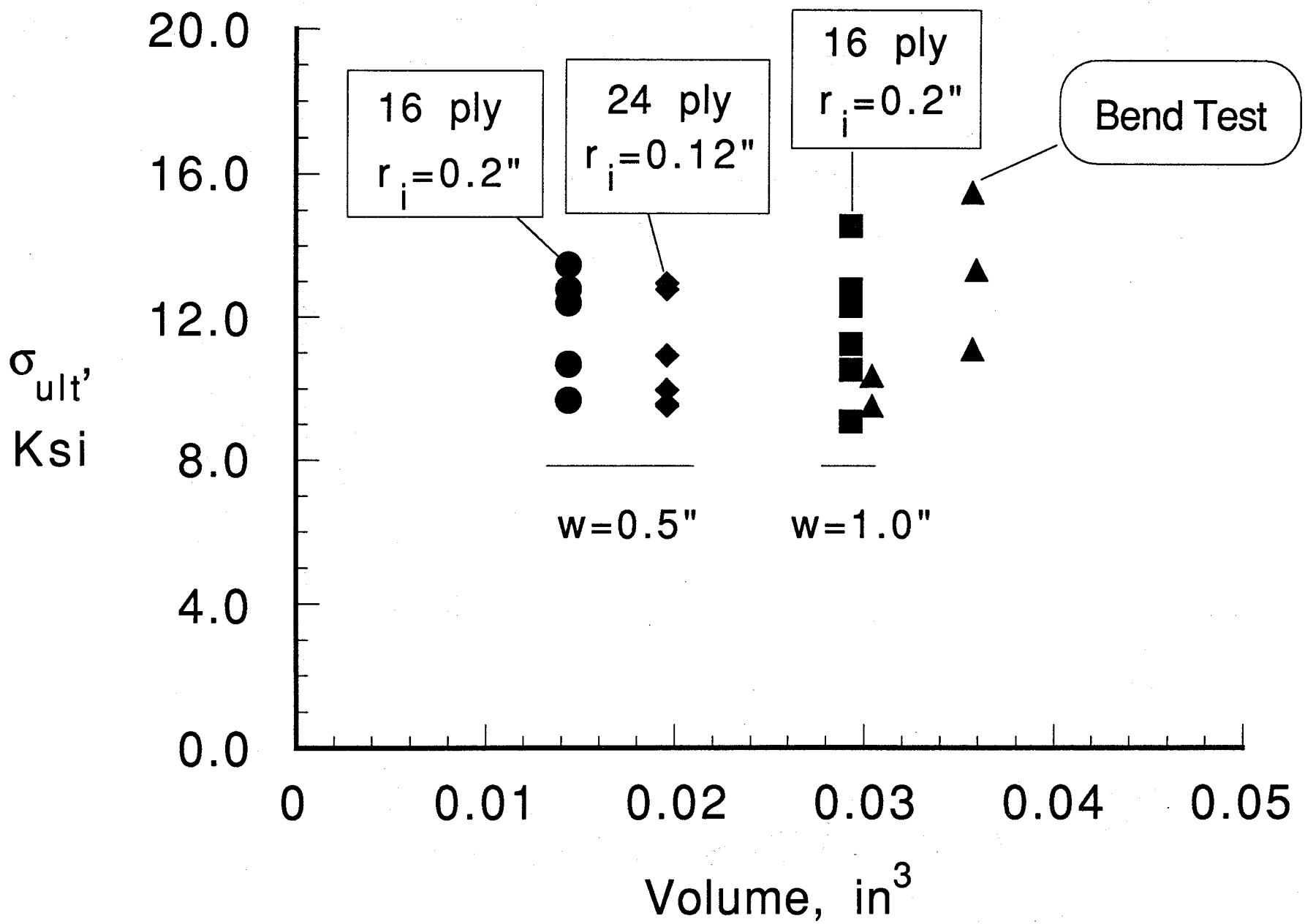

Figure 27 Transverse Tensile Strength of AS4/3501-6

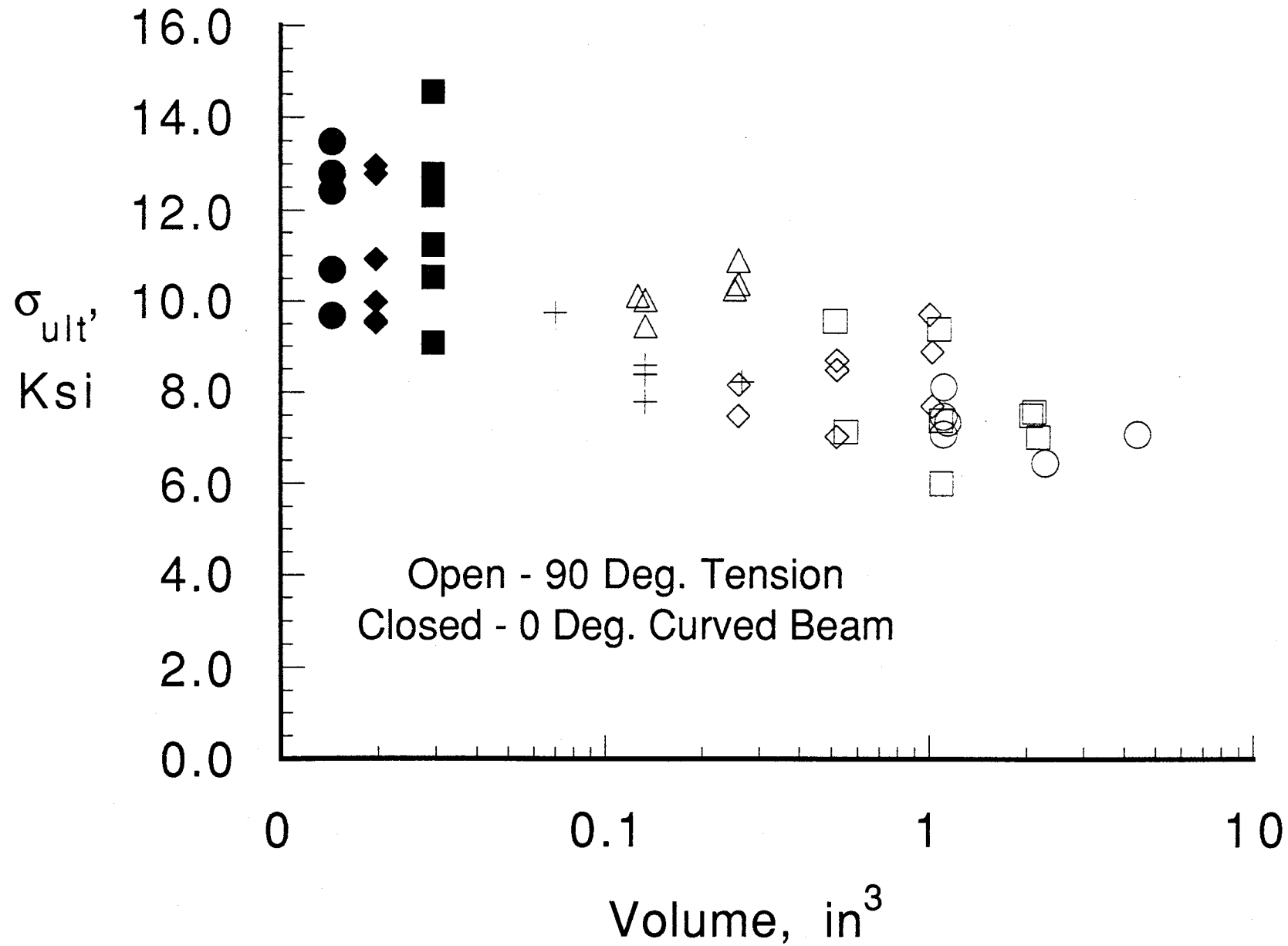

Figure 28 Predicted Interlaminar Tensile Strength
16-ply Zero Degree Curved Beam

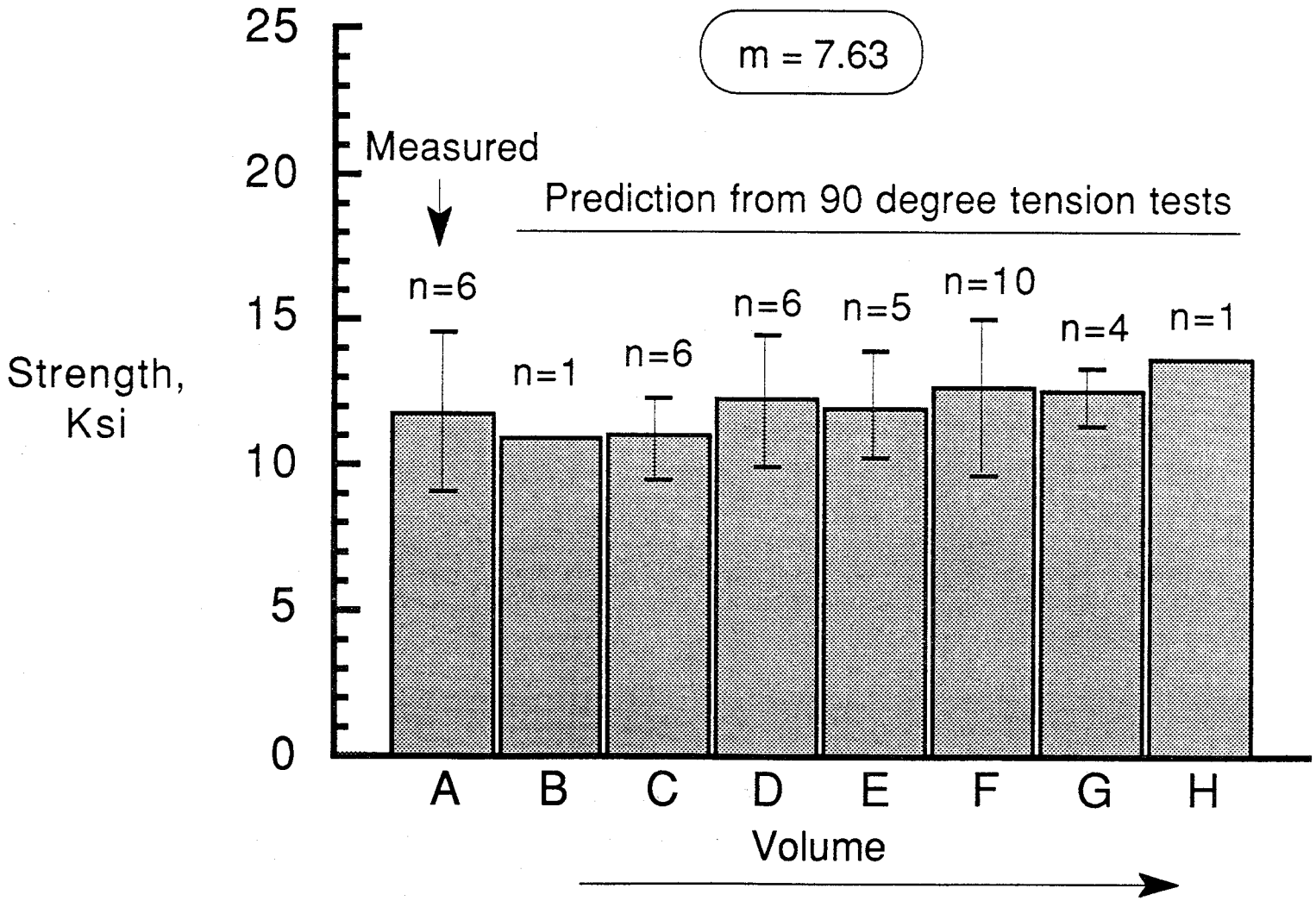

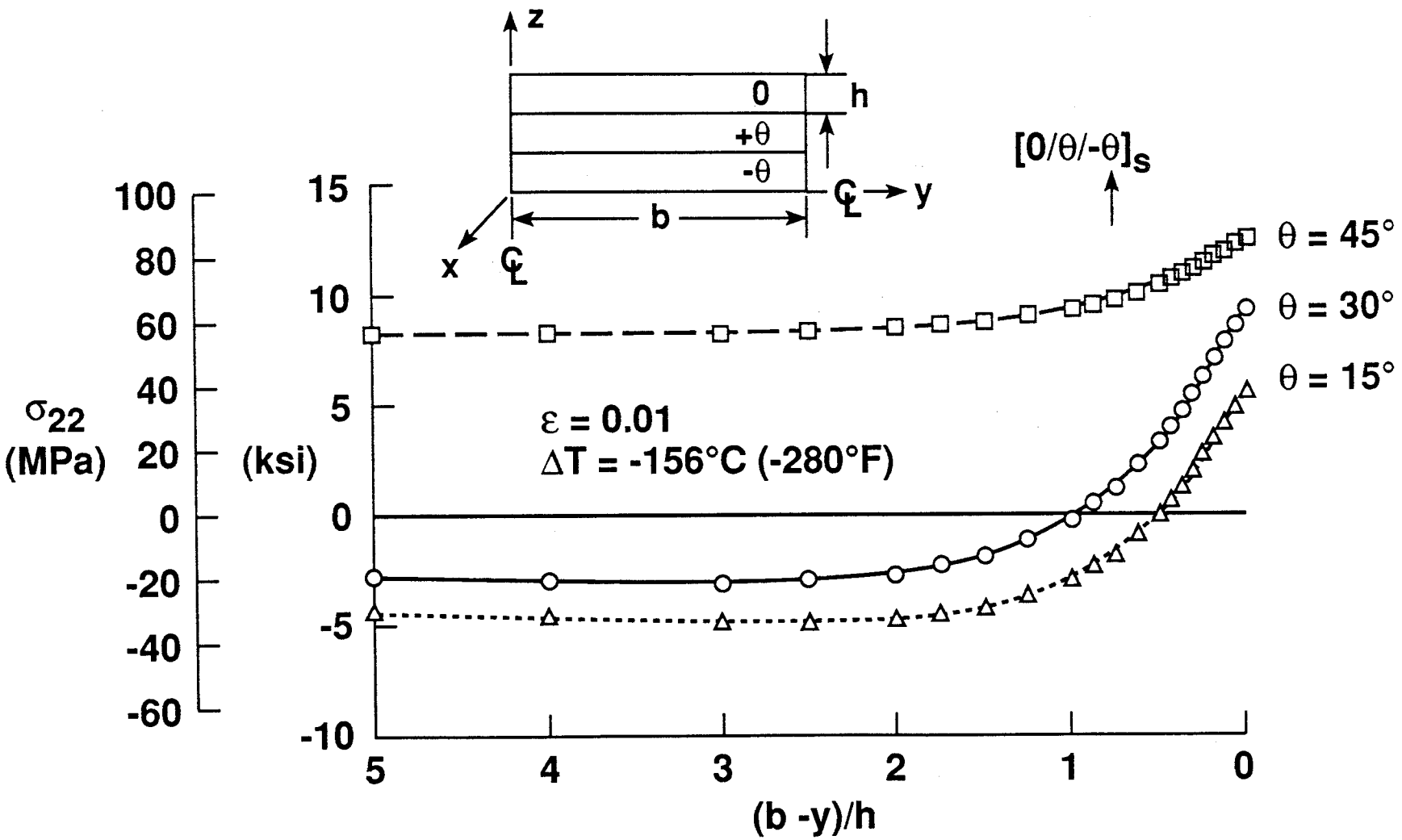

Figure 29. In-plane normal stress near the free edge of the -θ degree ply in $[0/\theta/-\theta]_s$ graphite epoxy laminate.

Figure 30 Influence of sample size on Characteristic Strength

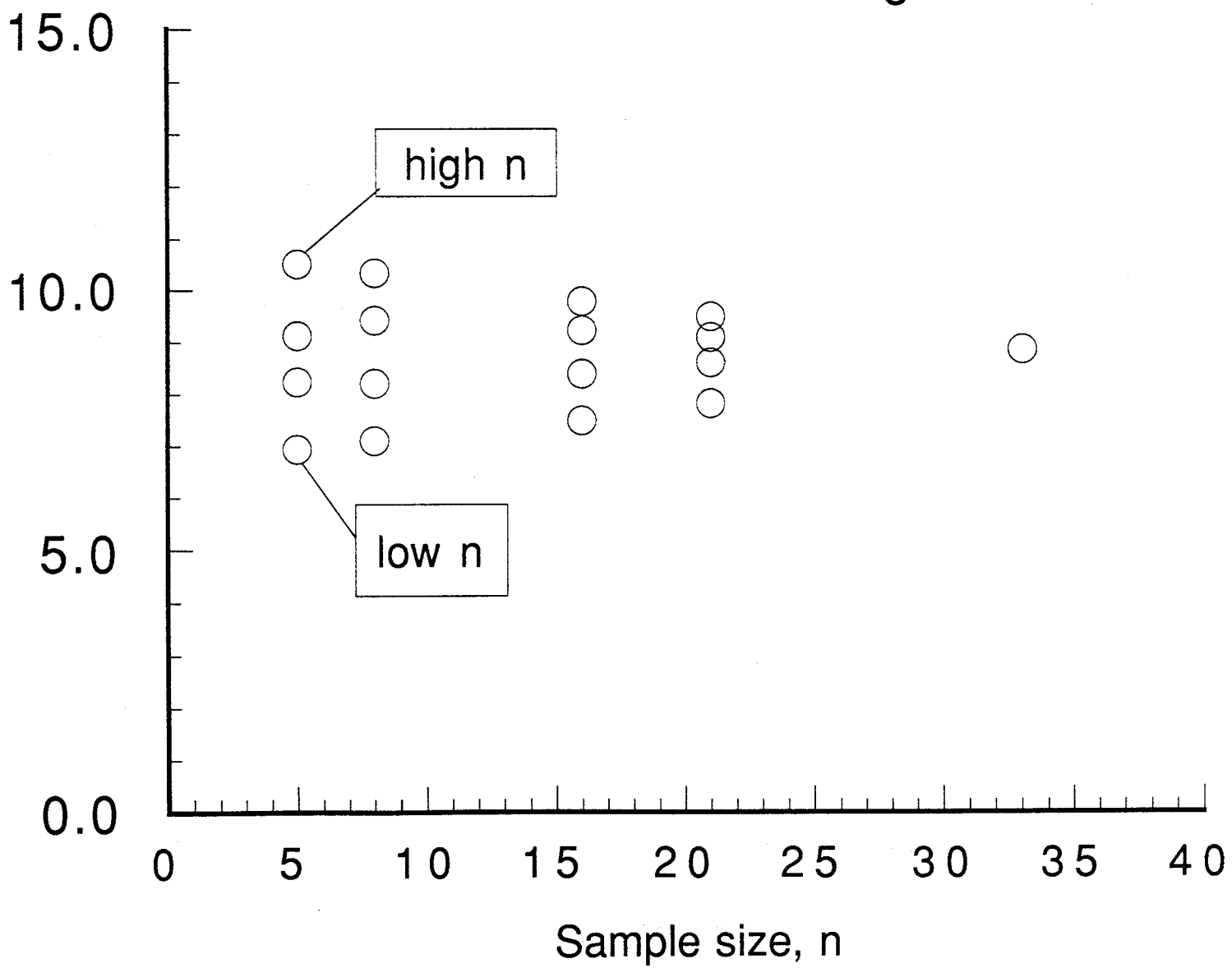

Figure 31 Influence of sample size on Weibull Shape Parameter

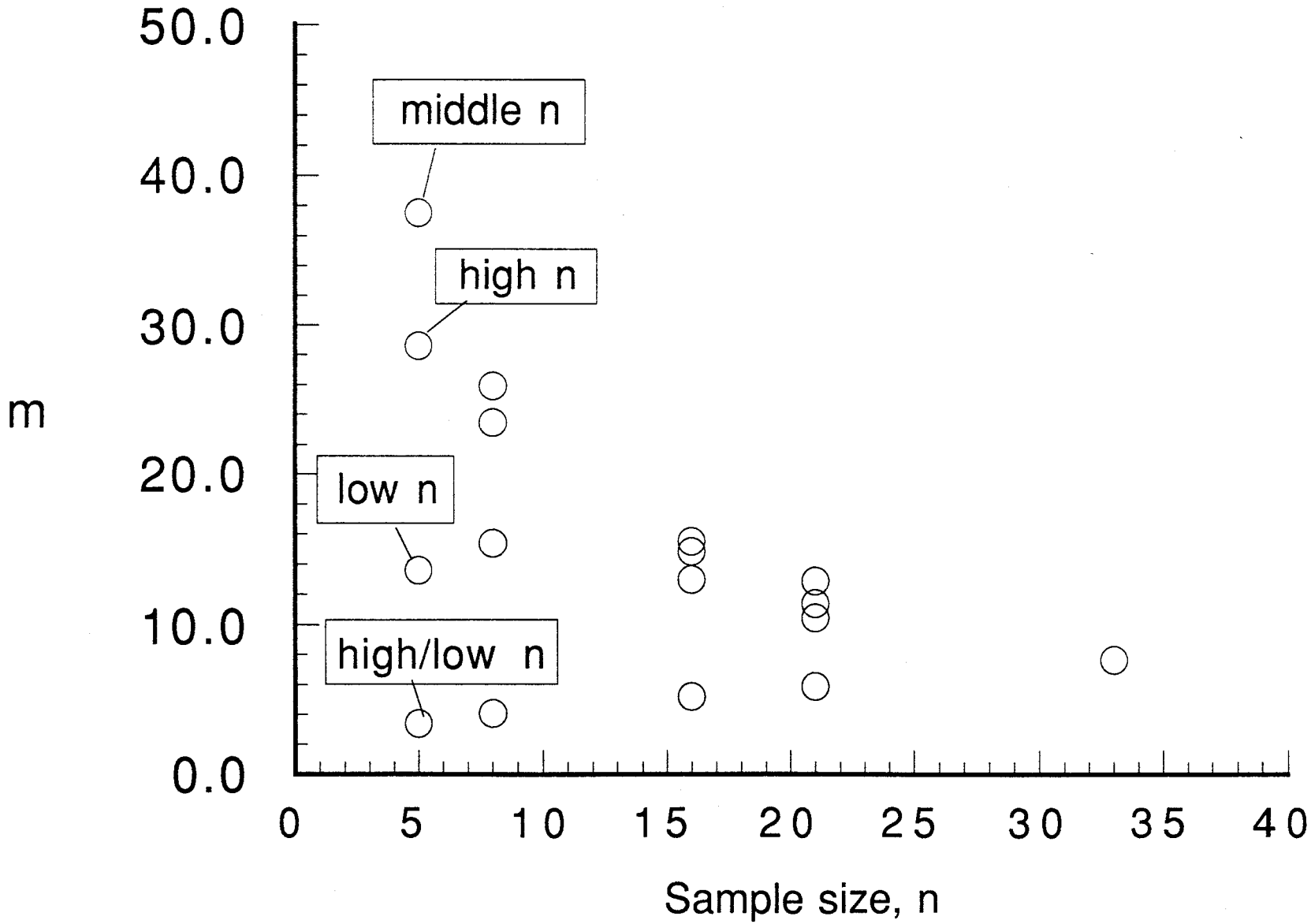

REPORT DOCUMENTATION PAGE

Form Approved
OMB No. 0704-0188

1. AGENCY USE ONLY (Leave blank)	2. REPORT DATE	3. REPORT TYPE AND DATES COVERED
	June 1992	Technical Memorandum

4. TITLE AND SUBTITLE
Scale Effects on the Transverse Tensile Strength of Graphite Epoxy Composites

5. FUNDING NUMBERS
505-63-50-04

6. AUTHOR(S)
T. Kevin O'Brien and Satish A. Salpekar

7. PERFORMING ORGANIZATION NAME(S) AND ADDRESS(ES)
Aerostructures Directorate
U.S. Army-AVSCOM
Langley Research Center
Hampton, VA 23665-5225

8. PERFORMING ORGANIZATION REPORT NUMBER

9. SPONSORING / MONITORING AGENCY NAME(S) AND ADDRESS(ES)
National Aeronautics and Space Administration
Washington, DC 20546-0001
and
U.S. Army Aviation Systems Command
St. Louis, MO 63120-1798

10. SPONSORING / MONITORING AGENCY REPORT NUMBER
NASA TM-107637
AVSCOM TR-92-B-009

11. SUPPLEMENTARY NOTES
O'Brien: U.S. Army Aerostructures Directorate, NASA Langley Research Center, Hampton, VA 23665-5225;
Salpekar: Analytical Services and Materials, Inc., NASA Langley Research Center, Hampton, VA 23665-5225

12a. DISTRIBUTION / AVAILABILITY STATEMENT
Unclassified - Unlimited

Subject Category - 24

12b. DISTRIBUTION CODE

13. ABSTRACT *(Maximum 200 words)*

The influence of material volume on the transverse tensile strength of AS4/3501-6 graphite epoxy composites was investigated. Tensile tests of 90 degree laminates with 3 different widths and 5 different thicknesses were conducted. A finite-element analysis was performed to determine the influence of the grip on the stress distribution in the coupons and explain the tendency for the distribution of failure locations to be skewed toward the grip. Specimens were instrumented with strain gages and extensometers to insure good alignment and to measure strains. Data indicated that matrix dominated strength properties varied with the volume of material that was stressed, with the strength decreasing as volume increased. Transverse strength data were used in a volumetric scaling law based on Weibull statistics to predict the strength of 90-degree laminates loaded in three point bending. Comparisons were also made between transverse strength measurements and out-of-plane interlaminar tensile strength measurements from curved beam bending tests. The significance of observed scale effects on the use of tests for material screening, quality assurance, and design allowables is discussed.

14. SUBJECT TERMS
Composite material; Graphite epoxy; Transverse tensile strength; Delamination; Matrix crack; Scale laws; Weibull statistics

15. NUMBER OF PAGES
59

16. PRICE CODE
A04

17. SECURITY CLASSIFICATION OF REPORT	18. SECURITY CLASSIFICATION OF THIS PAGE	19. SECURITY CLASSIFICATION OF ABSTRACT	20. LIMITATION OF ABSTRACT
Unclassified	Unclassified	Unclassified	